9

NUMERICAL TESTING OF ALGORITHM

9.1 INTRODUCTION

This chapter investigates the performance of a number of B-WIM algorithms (Chapter 7) with data from numerical (Chapter 5) and finite element simulations (Chapter 6). The interaction between bridge, trucks and road roughness involves many parameters which are difficult to identify and allow for when determining the static axle weights. As a result, the accuracy of B-WIM systems varies greatly. The B-WIM algorithms being tested are: traditional static (Section 3.3) with a new spectral calibration; dynamic B-WIM (Section 7.3) (both based on the instrumentation of one longitudinal section) and a static multiple-sensor approach based on many longitudinal locations (Section 7.5.2). Other algorithms have not been object of further consideration due to disadvantages given in Chapter 7. In this study, trucks and bridges are modelled through numerical and finite element approaches as described in Chapters 5 and 6 respectively.

Accuracy classes are determined according to the COST323 European Specification on WIM (Appendix B). Accuracy class for single axles or axles of a group are obtained strictly from the estimated weights provided by each algorithm. Then, individual axle weights are added together to obtain the weight of an axle group or the gross weight. Results for an axle in a group are generally very poor due to the difficulty of separating the individual contributions of each axle. For this reason the COST323 specification allows them to be omitted when classifying a B-WIM system. Accuracy for axles in a group may be improved by distributing the weight predicted for the whole group equally between axles, but it has been preferred to maintain the original axle values for evaluation purposes. Sections 9.2 and 9.3 will show how some algorithms can predict axles in a group accurately without any further manipulation. A calibration factor relates bending moment and change in voltage/strain and theoretically it should be independent of speed. Hence, a common calibration factor has been used for all speeds.

The first part of the chapter uses the numerical simulations provided by an independent source to assess B-WIM accuracy. Green (Queen's University, Kingston, Canada) calculates the strain output at five different locations of a one-dimensional bridge model. A two-axle vehicle is used for calibration. Once the system is calibrated, four-axle vehicles running with different loads, speeds and suspension types are weighed as their movement over the bridge is simulated. Two types of scenario are analysed: smooth and rough road profile. Guidance is provided for the estimation of the parameters governing the bridge behaviour. In the second part, different bridge finite element models are subjected to a common pattern of trucks to check their potential as B-WIM sites. The bridge characteristics appear to be a dominant factor for the accuracy of B-WIM systems. The influence of the sensor location on accuracy is also discussed.

9.2 TESTING WITH GREEN'S ONE DIMENSIONAL DYNAMIC INTERACTION MODEL

Green's one dimensional model has been described in Section 5.6. The bridge is 30 m long. Green calculates strain every 0.01 s (100 Hz) at 5, 10, 15, 20 and 25 m from the bridge support. The B-WIM system is calibrated by the author with a two-axle fully laden linear sprung vehicle (four degrees of freedom). Then, the author tests the system with a four-axle vehicle and two different suspension systems (air and steel leaf). The mechanical characteristics of this truck and the bridge model were not known to the author prior to the analysis. The static and dynamic (DB-WIM) algorithms are based on longitudinal bending at midspan, and the static multiple-sensor algorithm (MS-BWIM) on bending at five points equally spaced along the bridge. The calibration takes place in full repeatability conditions (r1) as defined in the COST323 specification (Appendix B): A two-axle vehicle passing at different speeds, one load and one lateral position on the road. Then, the system is tested in limited reproducibility conditions (R1): two 4-axle vehicles passing over the bridge at different speeds with different loads. Results are given for two different road profiles.

9.2.1 Calibration

The shape of the theoretical influence line is known from beam theory and the static algorithm only requires a calibration factor to adjust the magnitude of the strains to the theoretical model. If the exact influence line for bending moment is used, the calibration

factor is the product of the modulus of elasticity and the section modulus (Section 3.5.1 and Chapter 8 suggest an approach for obtaining the real shape of the influence line from an experimental record). For this analysis, the constant is obtained by dividing the real static gross vehicle weight by the predicted weight of the calibration truck. The calibration of DB-WIM requires additional dynamic parameters (natural frequency, damping) obtained from the record in free vibration. A linear sprung two axle vehicle with 4 m axle spacing, 32.42 kN static weight in the front axle and 59.94 kN in the rear axle is used for calibration.

Smooth Road Profile

At one particular location, bending moment is proportional to strain through the elasticity and section modulus (*ES*) as shown in Equation 3.1. Bending moment depends on the shape of the influence line, bridge length, static axle weights, axle spacings and position of the calibration vehicle. The results of the static calibration are shown in Figure 9.1.

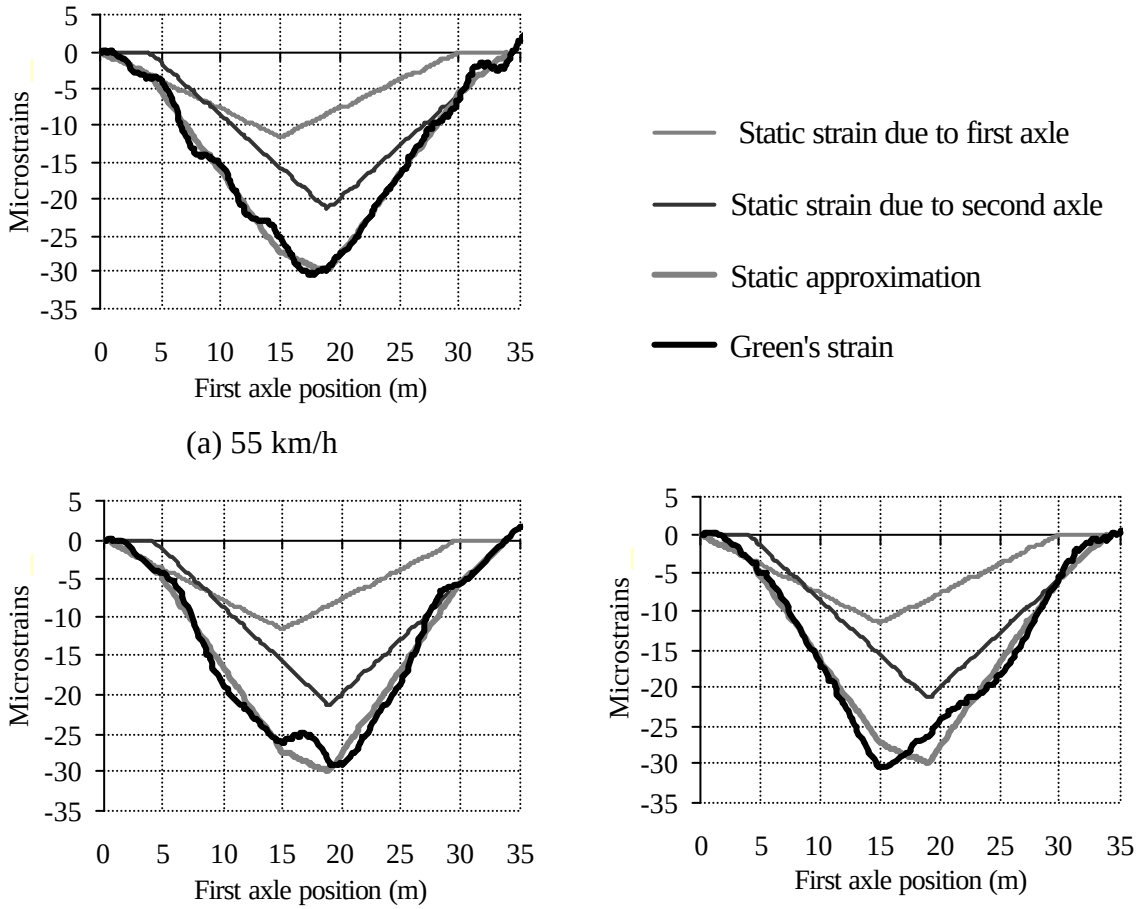

(a) 55 km/h

(b) 70 km/h

(c) 85 km/h

Figure 9.1 – Calibration of a static B-WIM algorithm (smooth profile)

The calibration factor changes for each speed very slightly (2.1056×10^{10} at 55 km/h, 2.1020×10^{10} at 70 km/h and 2.0812×10^{10} at 85 km/h). An average value of 2.0963×10^{10} is adopted.

Other sensor locations used for MS-BWIM are calibrated in the same way. The axle forces predicted by MS-BWIM are compared to the simulated applied forces in Figures 9.2(a) and (b). There is not a clear correspondence between predicted and simulated instantaneous wheel forces, but the average value is very similar in both cases. Dynamic wheel forces are strongly excited by a bump located at about 5 m from the bridge end. Values tend towards infinity at both ends of the instantaneous calculation (very small value of the determinant – Section 7.5.2) and they are not taken into account in the determination of the static weight.

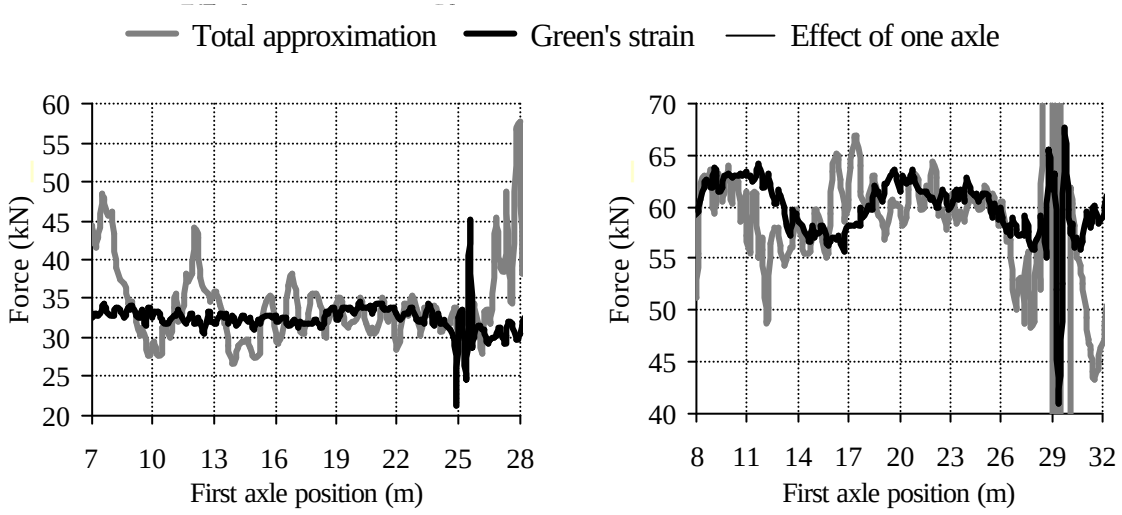

(a) Front axle (b) Rear axle

Figure 9.2 – History of axle forces for vehicle at 55 km/h (smooth profile)

Figure 9.3(a) shows the records in free vibration and Figure 9.3(b) the corresponding spectra for the three runs of the two-axle calibration vehicle. From these Figures, 0.97% damping and 3.33 Hz first natural frequency are obtained (The procedure for their determination is explained in Section 5.2.1).

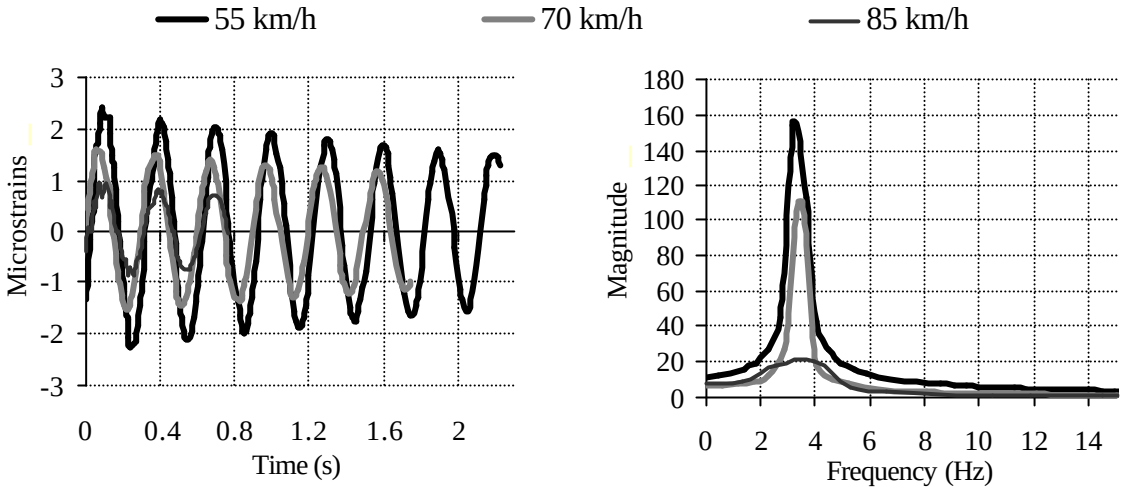

(a) Time Domain (b) Frequency Domain

Figure 9.3 – Record in free vibration (smooth profile)

The mass per unit length of the bridge is related to the first natural frequency through stiffness (*EI*) and bridge length (Equation 5.3). Section modulus, *S*, is related to second moment of area, *I*, by the distance from the deck soffit to the neutral axis, *y*. An initial estimate of *ES* is taken from the static algorithm. The static calibration at the lowest speed gives $ES=2.10564 \times 10^{10}$ (Figure 9.1(a)). A better estimate of the section modulus is expected at lower speeds as a higher number of dynamic oscillations will take place around the static response. Ideally, the best estimate of the section modulus would take place by positioning the vehicle statically on the bridge, but this is not always feasible. Tests have been carried out in the past to check the use of a stationary vehicle for calibration (Dempsey 1997). A calibration factor obtained from a strain record due to a vehicle travelling at a typical traffic speed gave better results, but this study used static equations instead of dynamic equations allowing for bridge vibration and damping (as proposed in Section 7.3).

The distance *y* from the measurement point to the neutral axis can be calculated by minimising an objective function given by the sum of squared differences between measured and theoretical strains. The procedure is represented in Figure 9.4.

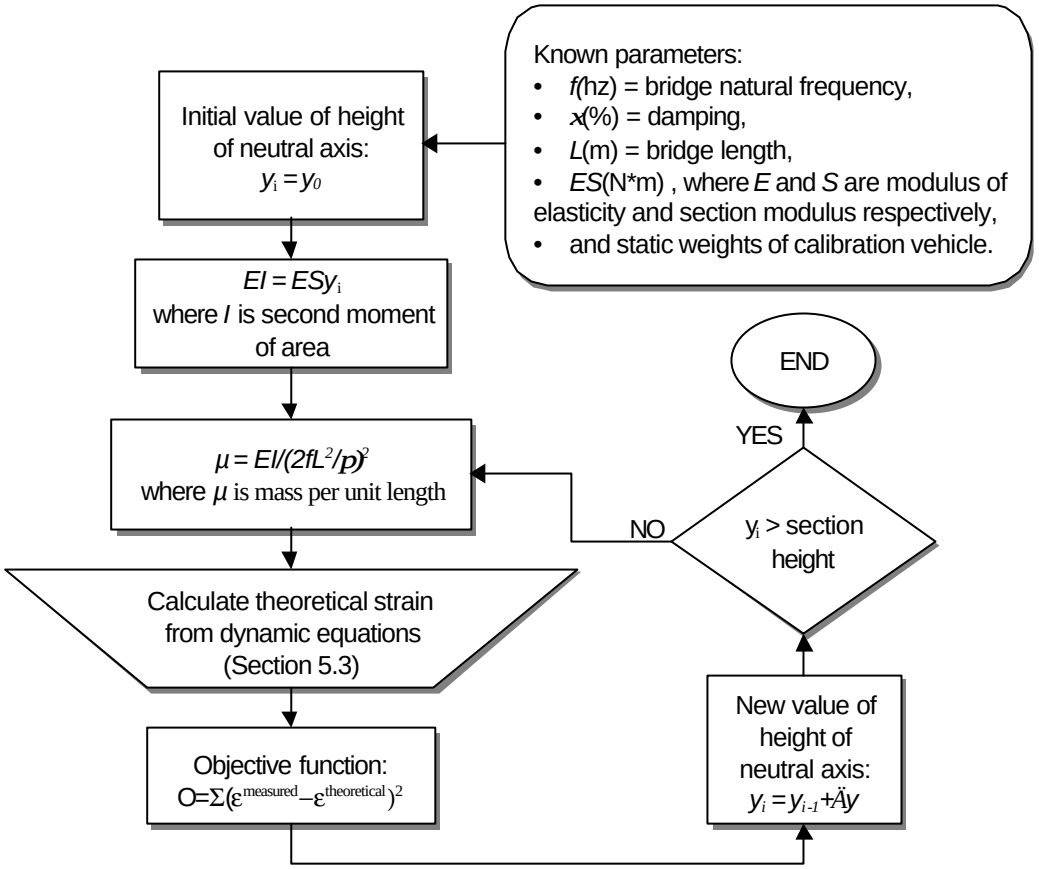

Figure 9.4 – Optimisation process for calculation of mechanical parameters

The values of the objective function for different y and speeds are given in Figures 9.5(a) and (b). From these curves, $y=2$ m. In practise (behaviour differing from beam theory), parameters other than y, i.e. mass per unit length μ, might also need to be optimised.

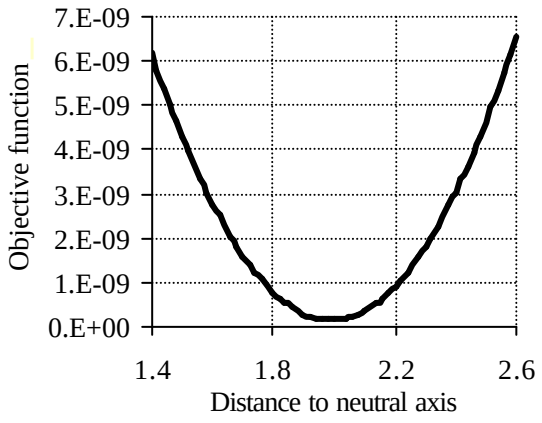

(a) Objective function at 55 km/h

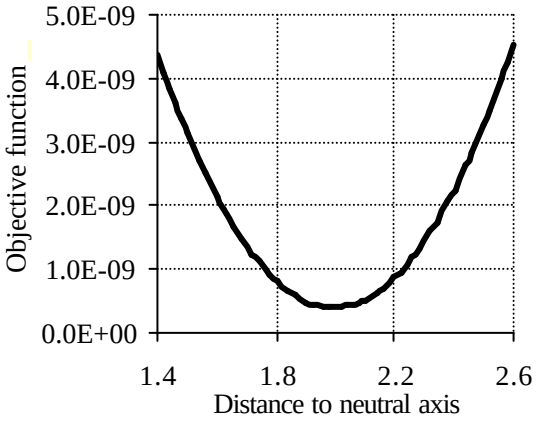

(b) Objective function at 85 km/h

Figure 9.5 – Determination of distance to the neutral axis (smooth profile)

Once the mechanical characteristics of the bridge are known, dynamic equations can be formulated for each speed (Section 5.3). The quality of the approximation of DB-WIM to the simulated response is shown in Figure 9.6.

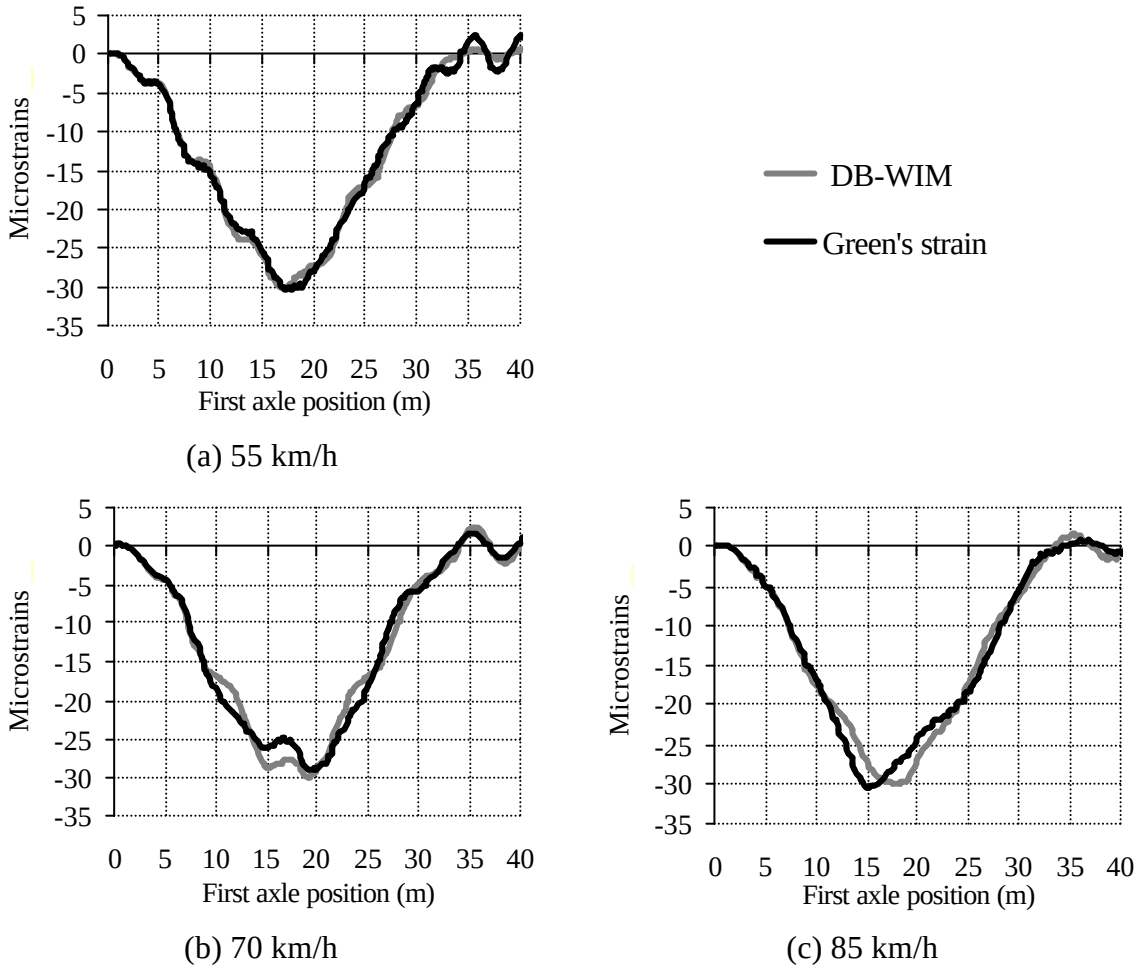

(a) 55 km/h

(b) 70 km/h

(c) 85 km/h

Figure 9.6 – Dynamic approximation (smooth profile)

Figure 9.7 illustrates the results in static weights for the calibration vehicle. The front axle is the lightest and the percentage error tends to be higher than in the rear axle as shown in Figures 9.7(b) and (c). DB-WIM and MS-BWIM are the most accurate algorithms for predicting gross weight and individual axle weights respectively. The traditional static B-WIM is also very accurate for gross vehicle weight. MS-BWIM is slightly worse for predicting gross vehicle weight, but the improvement in individual axle weights is very significant.

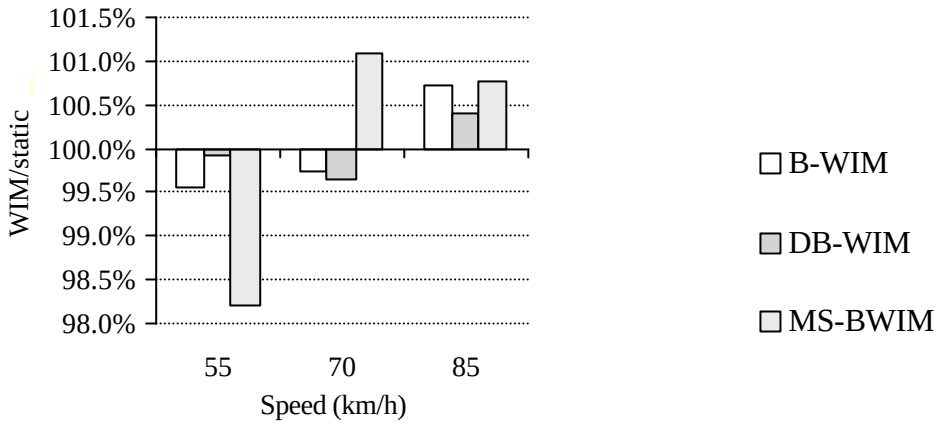

(a) Gross Weight

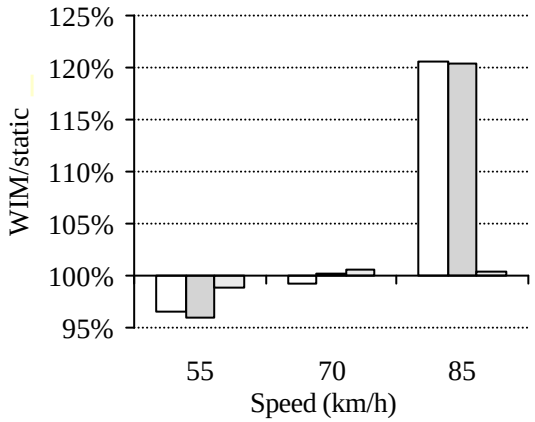

(b) Front axle

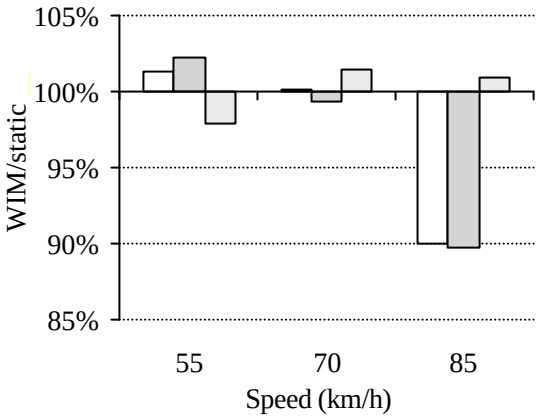

(c) Rear axle

Figure 9.7 – WIM/static weight versus speed (smooth profile)

Rough Road Profile

The calibration of the static algorithm is shown in Figure 9.8. The scale factor between real and predicted gross weight is 2.1197×10^{10} at 55 km/h, 2.1202×10^{10} at 70 km/h and 2.0839×10^{10} at 85 km/h. An average value of 2.0928×10^{10} is adopted as the calibration factor.

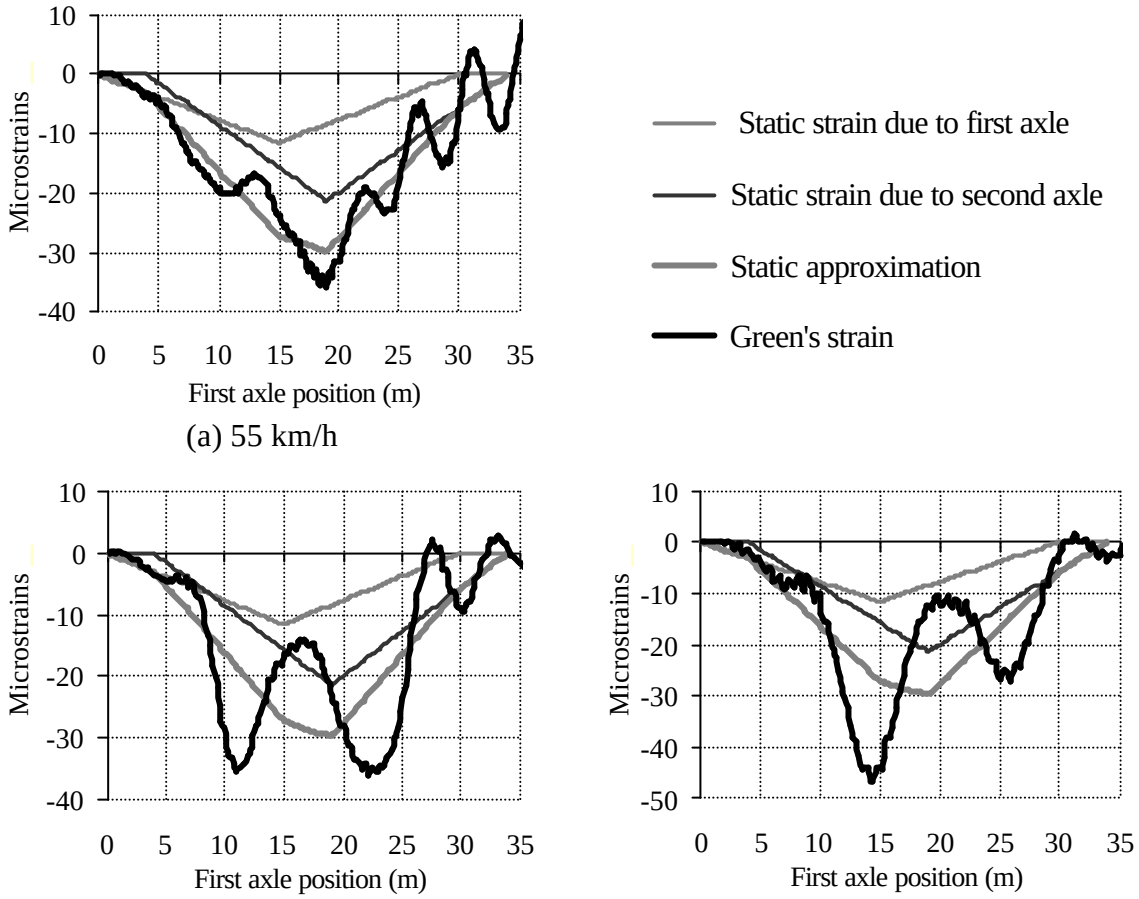

(a) 55 km/h

(b) 70 km/h

(c) 85 km/h

Figure 9.8 – Calibration of a static B-WIM algorithm (rough profile)

In the case of MS-BWIM, the prediction of instantaneous axle forces is not feasible throughout the bridge length. Figure 9.9 shows the results at 55 km/h.

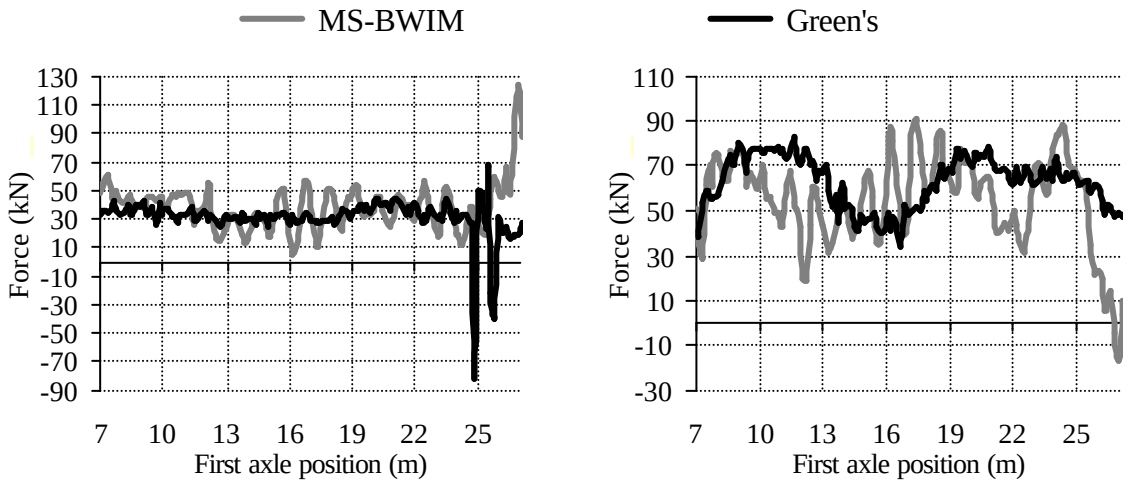

(a) Front axle

(b) Rear axle

Figure 9.9 - History of axle forces for vehicle at 55 km/h (rough profile)

As in the smooth road profile, the forces increase enormously at about 5 m from the bridge end and the instantaneous solution from here to the end of the record is ignored. There is a large increase in oscillations over the smooth case.

Figure 9.10 shows the variation of axle forces at 70 km/h. In Figure 9.10(b), the predicted answer for the rear axle exhibits a low frequency similar to that of the applied force.

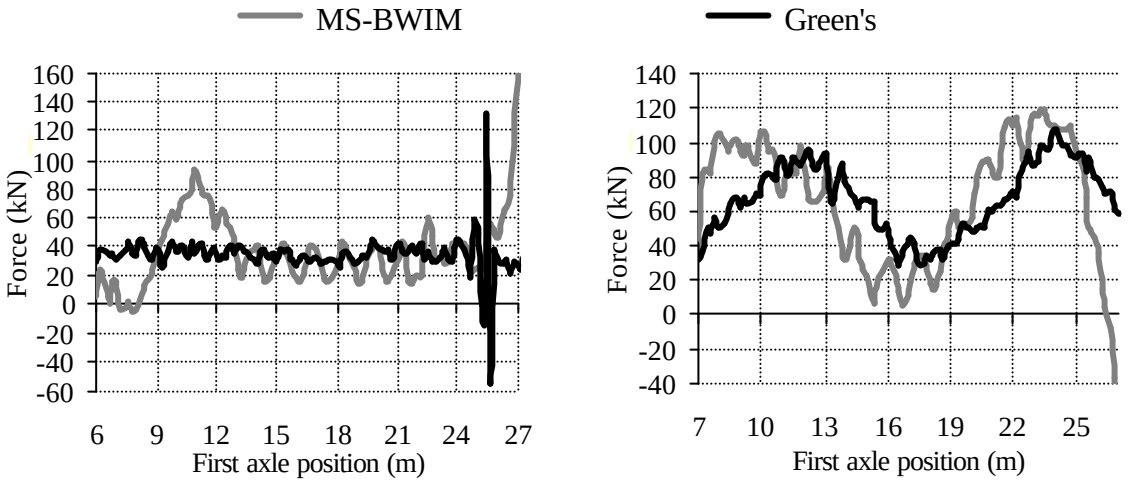

(a) Front axle (b) Rear axle

Figure 9.10 - History of axle forces for vehicle at 70 km/h (rough profile)

The prediction of the static answer proves more difficult at higher speeds, especially in the case of a rough profile. Figure 9.11 shows the calculation at 85 km/h. The estimate of the front axle is overweighed. MS-BWIM is not able to distinguish which is the force applied by each axle due to the strong dynamics and the limitation in the number of sensors. So, Figures 9.11(a) and (b) show how the prediction of the front axle follows a pattern similar to the simulated rear axle.

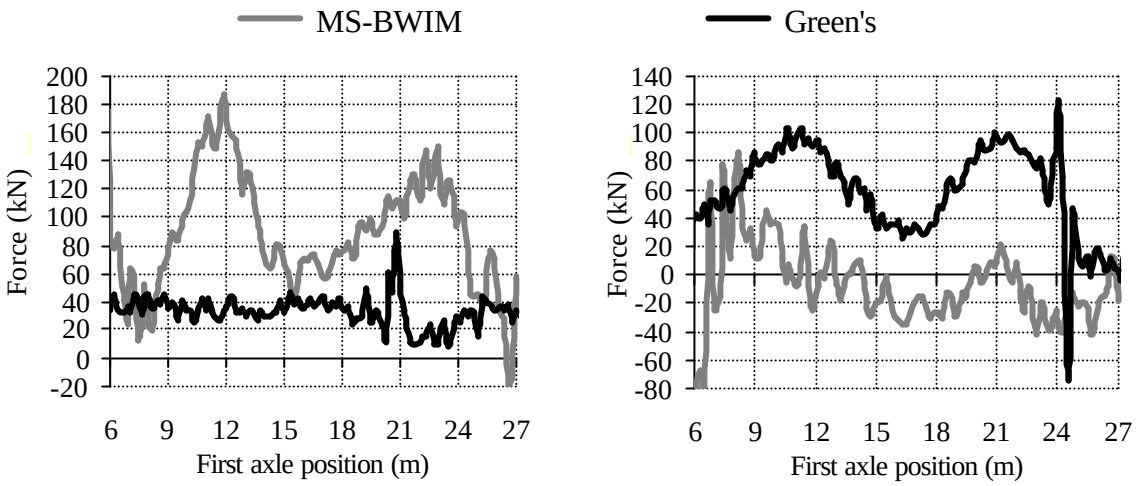

(a) Front axle (b) Rear axle

Figure 9.11 - History of axle forces for vehicle at 85 km/h (rough profile)

For the dynamic algorithm, section modulus is obtained from the run at 55 km/h (2.1197×10^{10}). The same dynamic characteristics as before are found for the bridge with rough road irregularities. From Figure 9.12(a): 3.33 Hz first natural frequency and 0.99% damping are obtained. Figure 9.12(b) represents the value of the objective function at 55 km/h, and the minimum takes place at a distance to the neutral axis of 2 m.

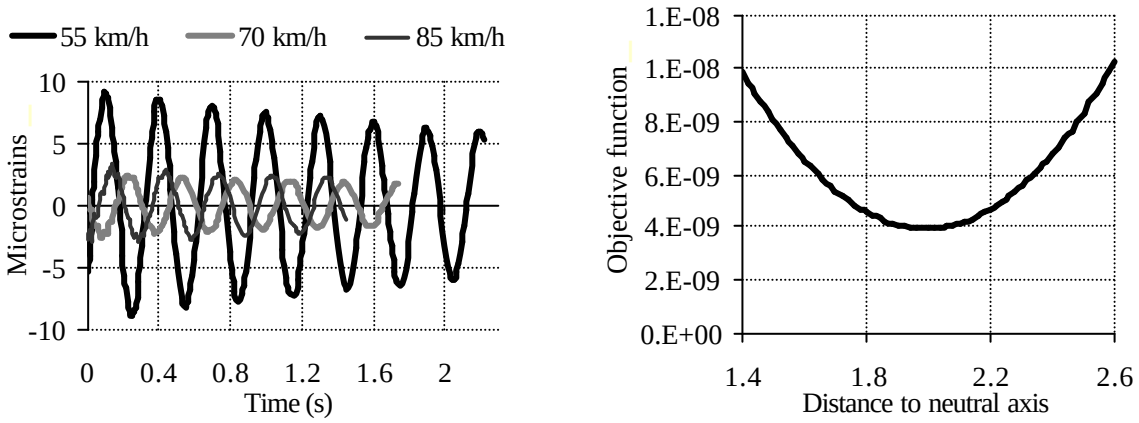

(a) Strain record in Free vibration (b) Distance to the neutral axis

Figure 9.12 – Determination of dynamic characteristics (rough profile)

The matching between the prediction by DB-WIM and the simulated response is shown for different speeds in Figure 9.13.

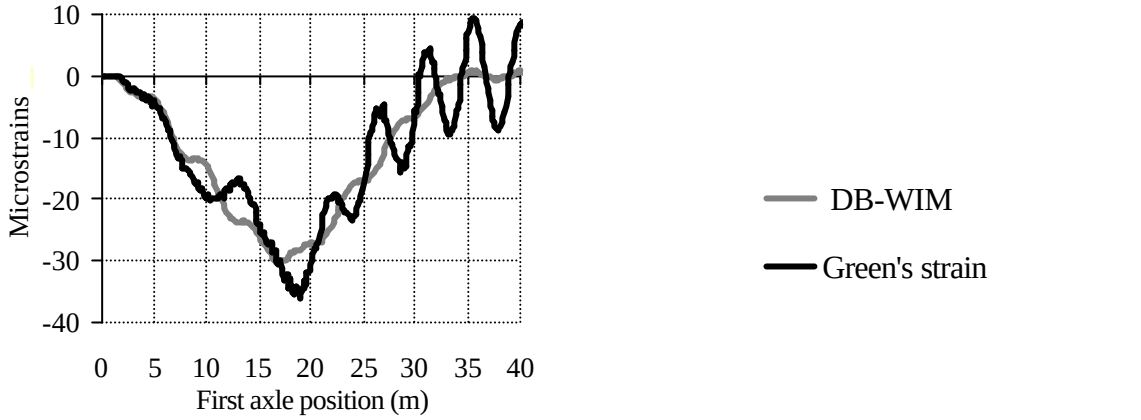

(a) 55 km/h

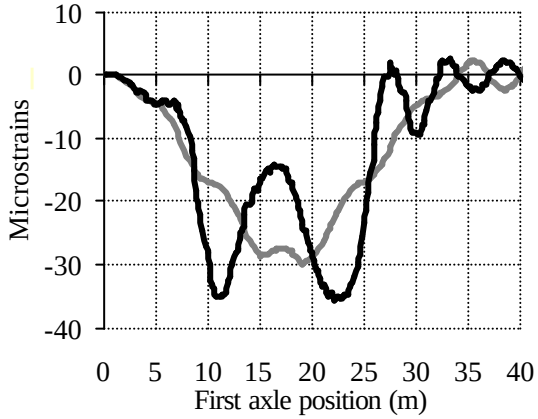

(b) 70 km/h

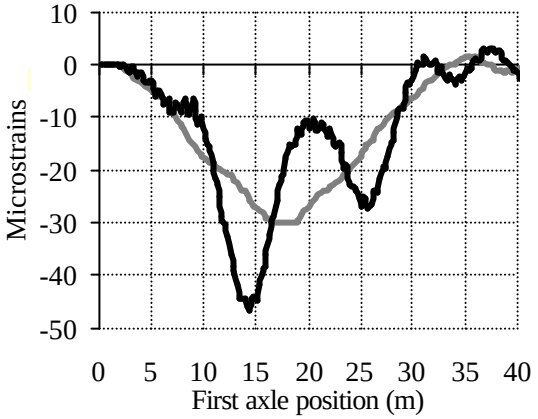

(c) 85 km/h

Figure 9.13 – Dynamic approximation (rough profile)

The errors in individual axle weights for the test vehicle are given in Figure 9.14. Calibration results are much poorer than in the case of a smooth profile (Figure 9.7). Results in individual axle weights at 85 km/h are very inaccurate, but static B-WIM and DB-WIM can predict gross weight within a small threshold.

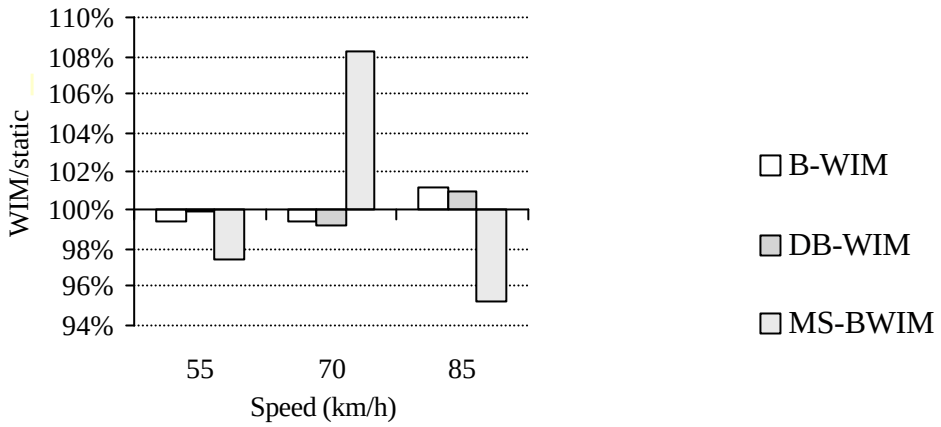

(a) Gross Weight

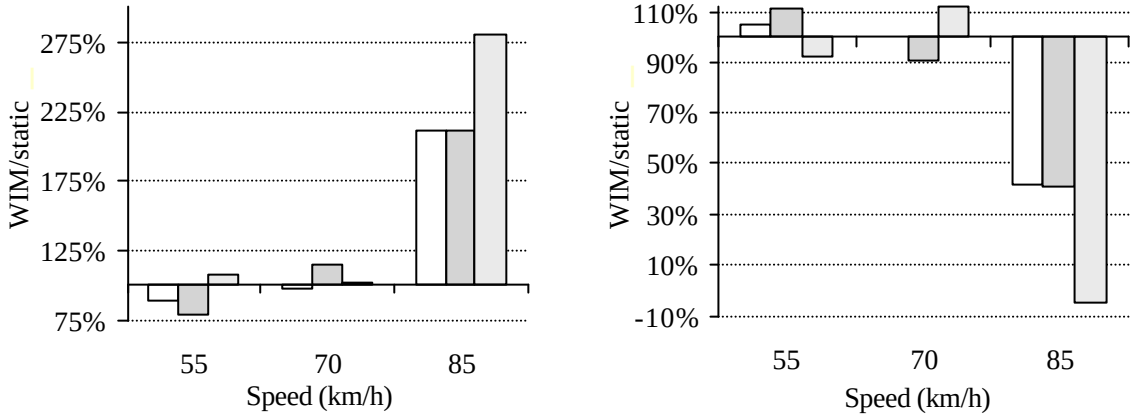

(a) Front axle (b) Rear axle

Figure 9.14 – WIM/static weight versus speed (rough profile)

9.2.2 Check of Accuracy

A four-axle vehicle (axle spacings 3.49, 6.76 and 2 m) is chosen for assessment of the initial calibration. The static weights of this vehicle were unknown to the author prior to the calculations. Two types of suspensions are investigated: air and steel leaf sprung. These two vehicles are driven at three different speeds (55, 70 and 85 km/h) and three loading conditions (unloaded, half and fully laden).

Smooth Road Profile

Figures 9.15 and 9.16 show the approximation by the static B-WIM and DB-WIM algorithms respectively, to the response caused by a fully laden 4-axle truck at 70 km/h.

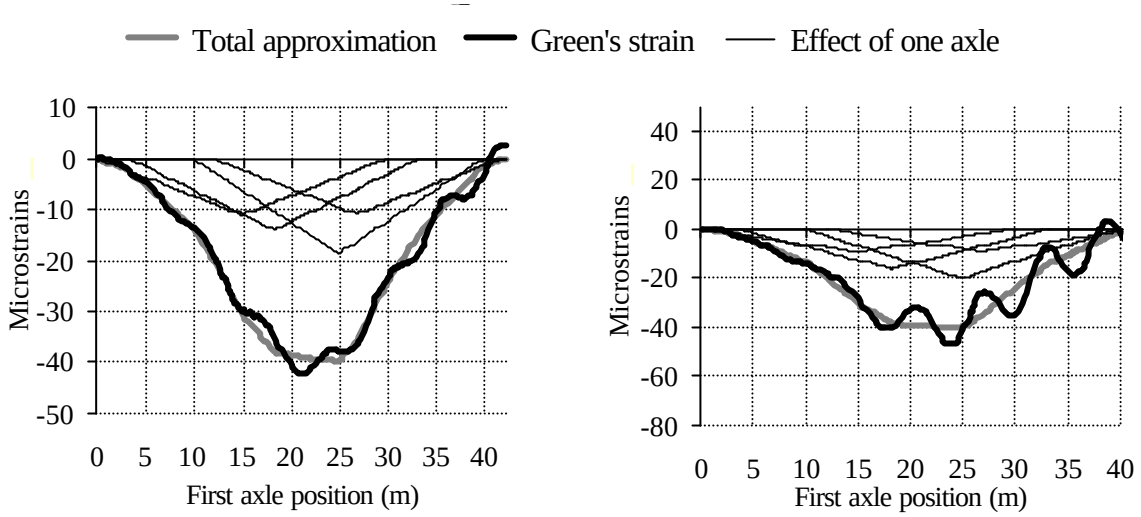

(a) Approximation for air suspension (b) Approximation for steel suspension

Figure 9.15 – Influence of suspension on static B-WIM (smooth profile)

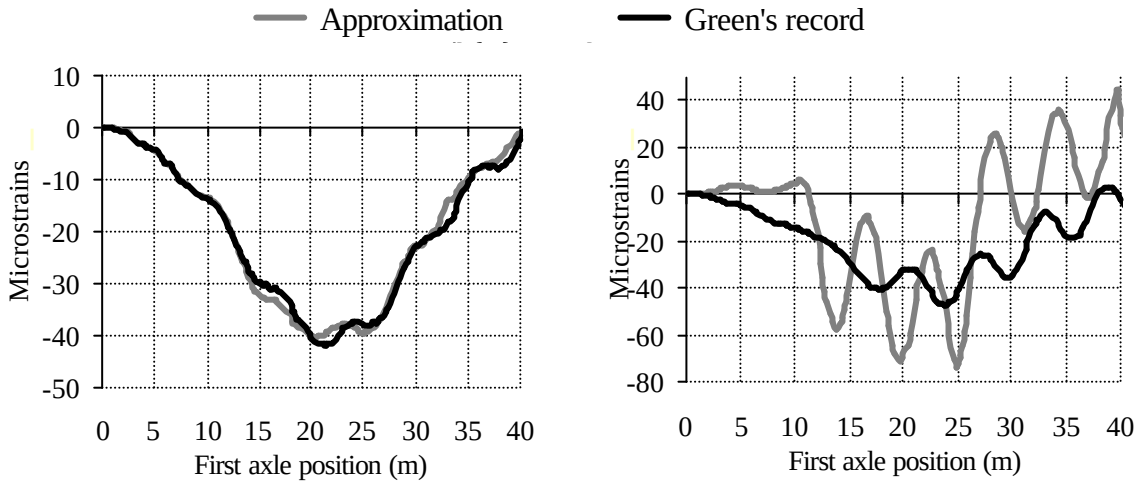

(a) Approximation for air suspension (b) Approximation for steel suspension

Figure 9.16 – Influence of suspension on DB-WIM (smooth profile)

The results illustrated in Figure 9.15 are based on the concept of an influence line, while Figure 9.16 is based on the dynamic answer due to a moving load. The strain record caused by a steel leaf suspension exhibits a higher deviation from the fitted response (by B-WIM or DB-WIM) than air suspension. Hence, predictions of individual axle weights are expected to be more accurate for air suspensions.

Figure 9.17 shows the simulated load history and the prediction by MS-BWIM for the case of a fully loaded 4-axle truck with air suspension travelling at 70 km/h. Figures 9.17(c)

and (d) show that the third and fourth axles allow for an instantaneous solution only when the first axle is located between 17 and 25 m from the bridge start.

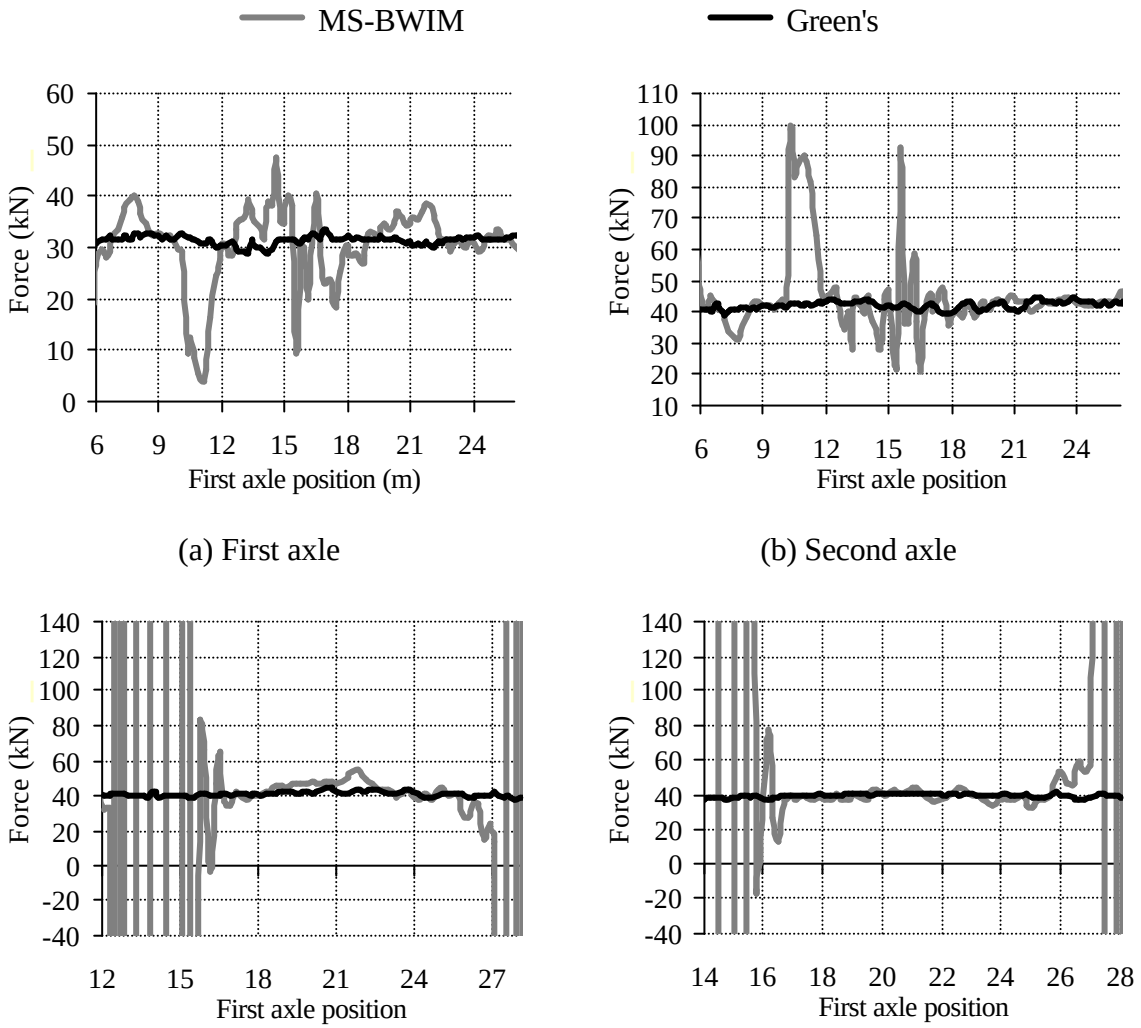

Figure 9.17 – Instantaneous calculation for leaf-sprung 4-axle truck (smooth profile)

Figure 9.18 shows the results of MS-BWIM when using the same truck and speed, but steel suspension. From Figures 9.17(c), 9.17(d), 9.18(c) and 9.18(d), the prediction of the third and fourth axles can be seen to be more difficult for the leaf sprung than the air sprung vehicle.

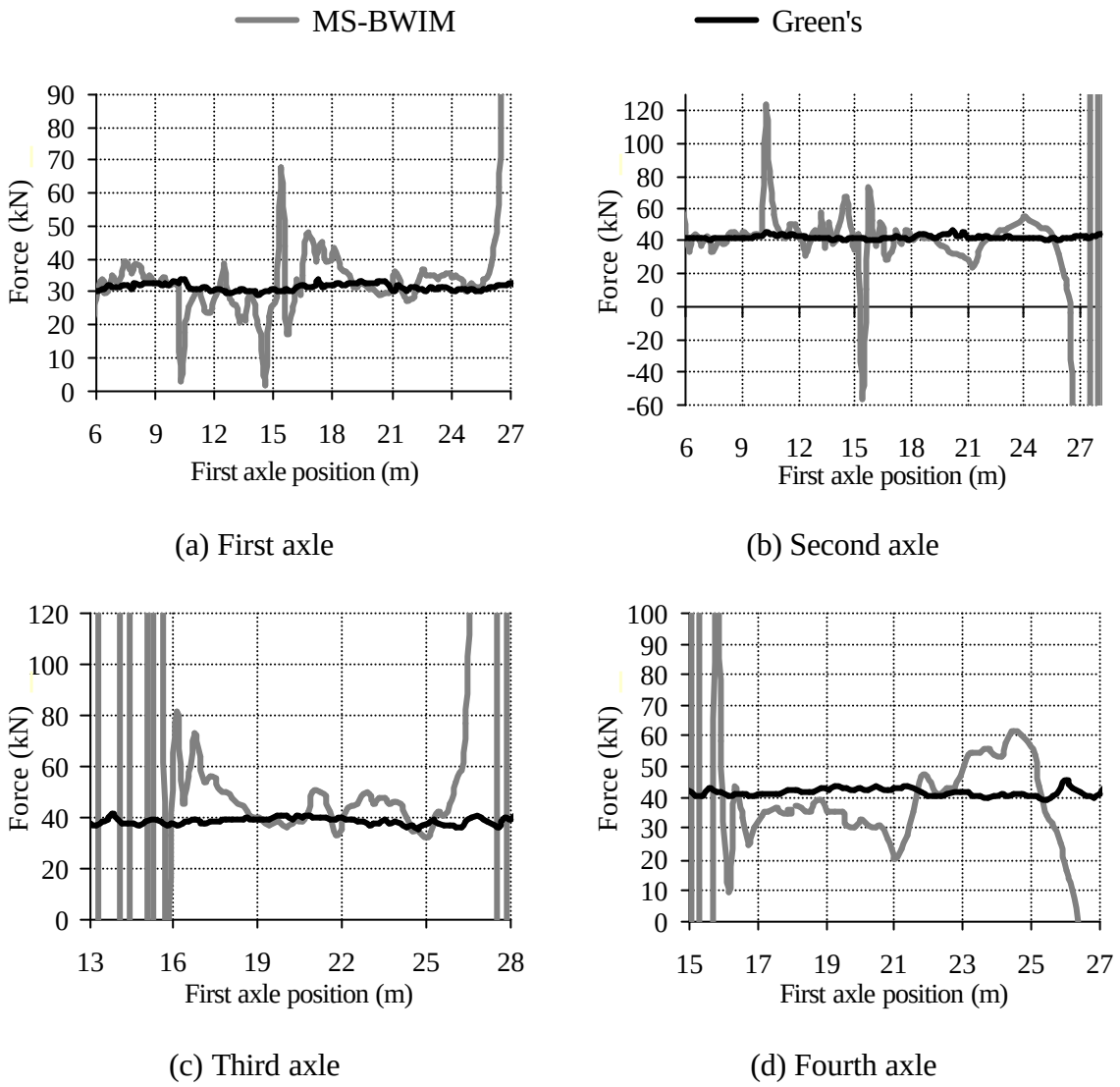

Figure 9.18 – Instantaneous calculation for steel sprung 4-axle truck (smooth profile)

Tables 9.1, 9.2 and 9.3 give accuracy classes for each criterion and algorithm. MS-BWIM is very accurate for all single criteria, even axles of a group in class B(10). The static B-WIM algorithm can predict gross weight accurately (A(5)), but fails to predict single axles (E(45)). DB-WIM is not as accurate as the static B-WIM or MS-BWIM.

Table 9.1 – Accuracy classification for static B-WIM algorithm (beam model) (R1)

(**n**: Total number of vehicles; **m**: mean; **s**: Standard deviation; $\mathbf{p_0}$: level of confidence; **d**: tolerance of the retained accuracy class; $\mathbf{d_{min}}$: minimum width of the confidence interval for π_0; **p**: Level of confidence of the interval $[-\delta,\delta]$)

	Relative error statistics				Accuracy calculation				
Criterion	**n**	**m (%)**	**s (%)**	**p_o (%)**	**Class**	**d (%)**	**d_{min} (%)**	**p (%)**	**Class Retained**
Single axle	36	-0.31	21.36	93.1	**E(45)**	54	47.3	96.5	**E(45)**
Group of axles	18	-2.34	7.71	90.3	**C(15)**	18	17.9	90.5	
Gross Weight	18	-0.79	0.93	90.3	**A(5)**	5	2.5	100.	

Table 9.2 – Accuracy classification for DB-WIM algorithm (beam model) (R1)

(**n**: Total number of vehicles; **m**: mean; **s**: Standard deviation; $\mathbf{p_0}$: level of confidence; **d**: tolerance of the retained accuracy class; $\mathbf{d_{min}}$: minimum width of the confidence interval for π_0; **p**: Level of confidence of the interval $[-\delta,\delta]$)

	Relative error statistics				Accuracy calculation				
Criterion	**n**	**m (%)**	**s (%)**	**p_o (%)**	**Class**	**d (%)**	**d_{min} (%)**	**p (%)**	**Class Retained**
Single axle	36	5.27	30.57	93.1	**E(65)**	78	68.4	96.4	**E(65)**
Group of axles	18	-7.80	11.88	90.3	**E(30)**	33	30.3	93.4	
Gross Weight	18	0.27	2.63	90.3	**B+(7)**	7	5.9	95.5	

Table 9.3 – Accuracy classification for static MS-BWIM algorithm (beam model) (R1)

(**n**: Total number of vehicles; **m**: mean; **s**: Standard deviation; $\mathbf{p_0}$: level of confidence; **d**: tolerance of the retained accuracy class; $\mathbf{d_{min}}$: minimum width of the confidence interval for π_0; **p**: Level of confidence of the interval $[-\delta,\delta]$)

	Relative error statistics				Accuracy calculation				
Criterion	**n**	**m (%)**	**s (%)**	**p_o (%)**	**Class**	**d (%)**	**d_{min} (%)**	**p (%)**	**Class Retained**
Single axle	36	-0.89	3.74	93.1	**B+(7)**	11	8.5	98.3	**B(10)**
Axle of group	36	-0.32	8.31	93.1	**B(10)**	20	18.4	95.4	
Group of axles	18	-0.07	2.70	90.3	**A(5)**	7.14	6.1	95.3	
Gross Weight	18	-0.56	1.46	90.3	**A(5)**	5	3.4	98.8	

If only the runs of the air suspension truck are taken into account, accuracy classes in the new *extended repeatability* conditions (r2) get worse for all algorithms except the dynamic B-WIM as shown in Tables 9.4, 9.5 and 9.6 (While the COST323 specification aims to

allow for differences in test conditions, extended repeatability proves in this case to be a more rigorous test for the algorithms. In any event, as it is more representative, the results for extended repeatability conditions are more relevant than for full repeatability).

Table 9.4 – Accuracy classification for static B-WIM algorithm (beam, air susp.) (r2)

(**n**: Total number of vehicles; **m**: mean; **s**: Standard deviation; $\mathbf{p_0}$: level of confidence; **d**: tolerance of the retained accuracy class; $\mathbf{d_{min}}$: minimum width of the confidence interval for π_0; **p**: Level of confidence of the interval $[-\delta,\delta]$)

	Relative error statistics				Accuracy calculation				
Criterion	**n**	**m (%)**	**s (%)**	**p_0 (%)**	**Class**	**d (%)**	**d_{min} (%)**	**p (%)**	**Class Retained**
Single axle	18	-0.71	20.17	93.7	**E(50)**	60	50.3	97.6	**E(50)**
Group of axles	9	-1.40	8.44	88.8	**D+(20)**	23	21.7	91.1	
Gross Weight	9	-0.76	0.54	88.8	**A(5)**	5	1.9	100.	

Table 9.5 – Accuracy classification for DB-WIM (beam, air suspension) (r2)

(**n**: Total number of vehicles; **m**: mean; **s**: Standard deviation; $\mathbf{p_0}$: level of confidence; **d**: tolerance of the retained accuracy class; $\mathbf{d_{min}}$: minimum width of the confidence interval for π_0; **p**: Level of confidence of the interval $[-\delta,\delta]$)

	Relative error statistics				Accuracy calculation				
Criterion	**n**	**m (%)**	**s (%)**	**p_0 (%)**	**Class**	**d (%)**	**d_{min} (%)**	**p (%)**	**Class Retained**
Single axle	18	2.47	24.22	93.7	**E(60)**	72	60.5	97.5	**E(60)**
Group of axles	9	-6.11	10.86	88.8	**E(30)**	33	30.0	92.6	
Gross Weight	9	-0.65	0.67	88.8	**A(5)**	5	2.1	100.	

Table 9.6 – Accuracy classification for static MS-BWIM (beam, air suspension) (r2)

(**n**: Total number of vehicles; **m**: mean; **s**: Standard deviation; $\mathbf{p_0}$: level of confidence; **d**: tolerance of the retained accuracy class; $\mathbf{d_{min}}$: minimum width of the confidence interval for π_0; **p**: Level of confidence of the interval $[-\delta,\delta]$)

	Relative error statistics				Accuracy calculation				
Criterion	**n**	**m (%)**	**s (%)**	**p_0 (%)**	**Class**	**d (%)**	**d_{min} (%)**	**p (%)**	**Class Retained**
Single axle	18	-1.81	2.56	93.7	**A(5)**	8	7.3	96.2	**C(15)**
Axle of group	18	0.40	8.64	93.7	**C(15)**	25	21.5	97.2	
Group of axles	9	0.71	2.91	88.8	**B+(7)**	10	7.6	96.9	
Gross Weight	9	-0.69	1.60	88.8	**A(5)**	5	4.3	94.3	

All results are represented in Figure 9.19. In comparison with the calibration, the bias on the single axle loads have been multiplied by factors of 0.75, 4.2 and 89 in the static, dynamic and multiple-sensor algorithms respectively, while the standard deviations have increased by more than 100%.

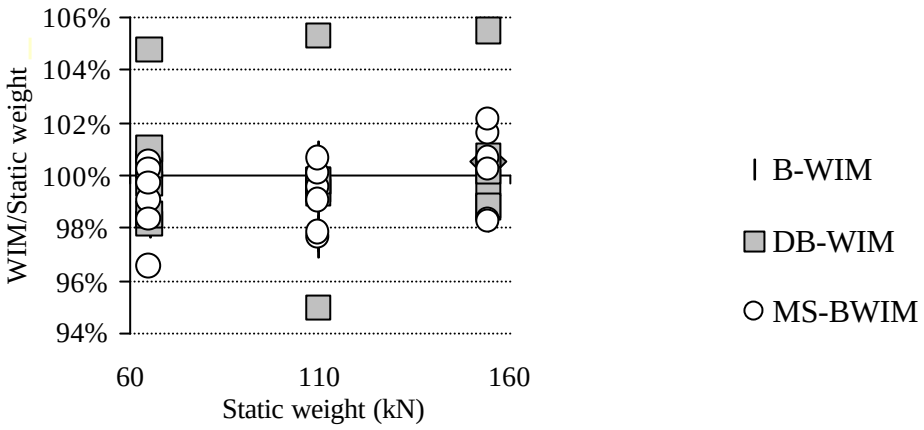

(a) Gross vehicle weight

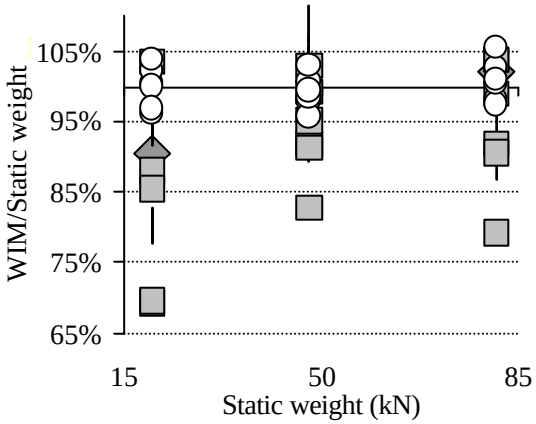

(b) Axle group

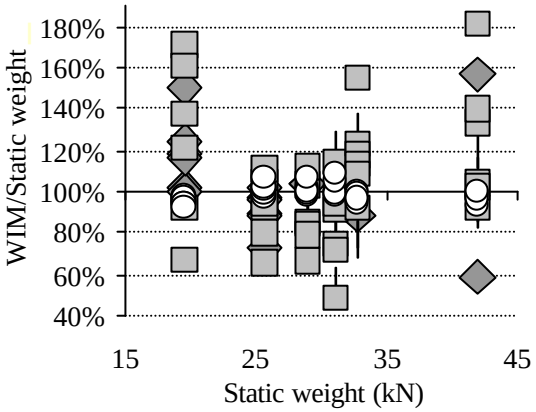

(c) Individual axle weights

Figure 9.19 – WIM/Static versus real static weights

Rough Road Profile

Results for a rough road profile are very poor and only gross weight give sensible levels of accuracy. The poor accuracy of a B-WIM algorithm on a rough profile can be explained by Figures 9.20 and 9.21. Figure 9.20 represents the approximation by the static algorithm to the total strain generated by a fully laden truck at 70 km/h. The total response is far from this static response due to the high dynamic oscillations.

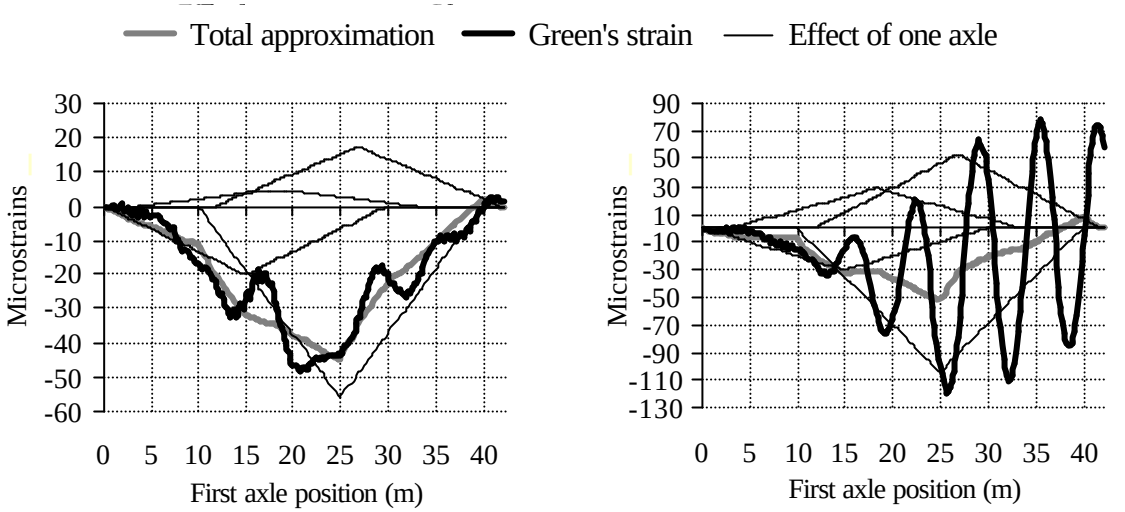

(a) Approximation for air suspension (b) Approximation for steel suspension

Figure 9.20 – Influence of suspension type on static B-WIM (rough profile)

Likewise Figure 9.21 represents the adjustment by DB-WIM. Both static and dynamic algorithms are very inaccurate and their approximations can lead to negative values for individual axle weights: For instance, the second and fourth axles in Figures 9.20(a) and (b) (thin line representing bending moment diagram due to a single axle is over the x-axis). the fourth axle from calculations by DB-WIM in Figure 9.21(a), and the first and fourth axles in Figure 9.21(b). As in the case of a smooth profile, steel leaf suspensions give worse results than air suspensions.

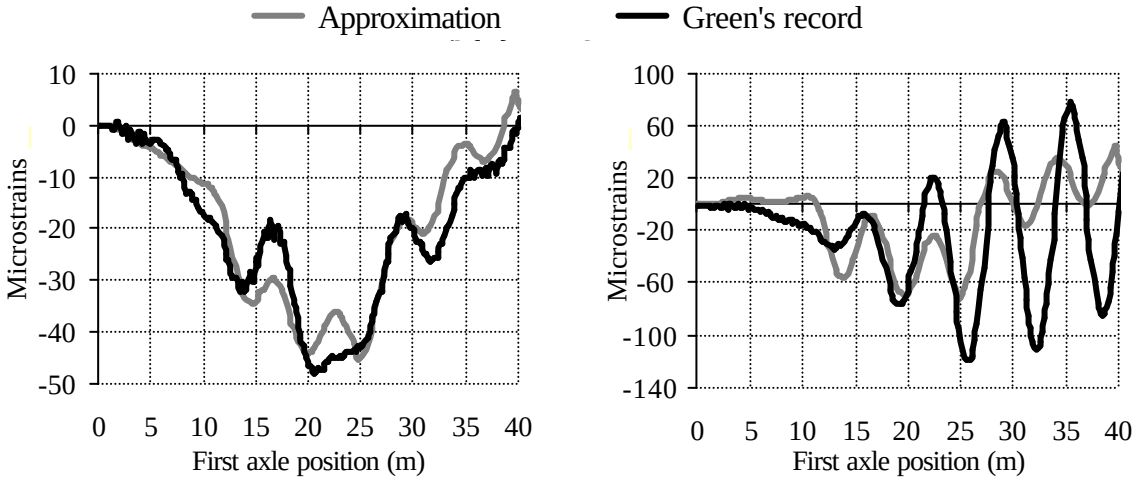

(a) Approximation for air suspension (b) Approximation for steel suspension

Figure 9.21 – Influence of suspension type on DB-WIM (rough profile)

If the road is in a poor condition, algorithms based on linearity and superposition do not appear to offer a valid solution. MS-BWIM is also extremely inaccurate as it minimises the instantaneous solution by using influence lines at many locations. Figure 9.22 shows the results for the same run as Figures 9.20(a) and 9.21(a). The static value can be estimated from instantaneous values when the first axle is located between 18 and 25 m from the bridge start. However, the third axle and fourth axles are strongly overweighed and underweighed respectively (Figures 9.22(c) and (d)).

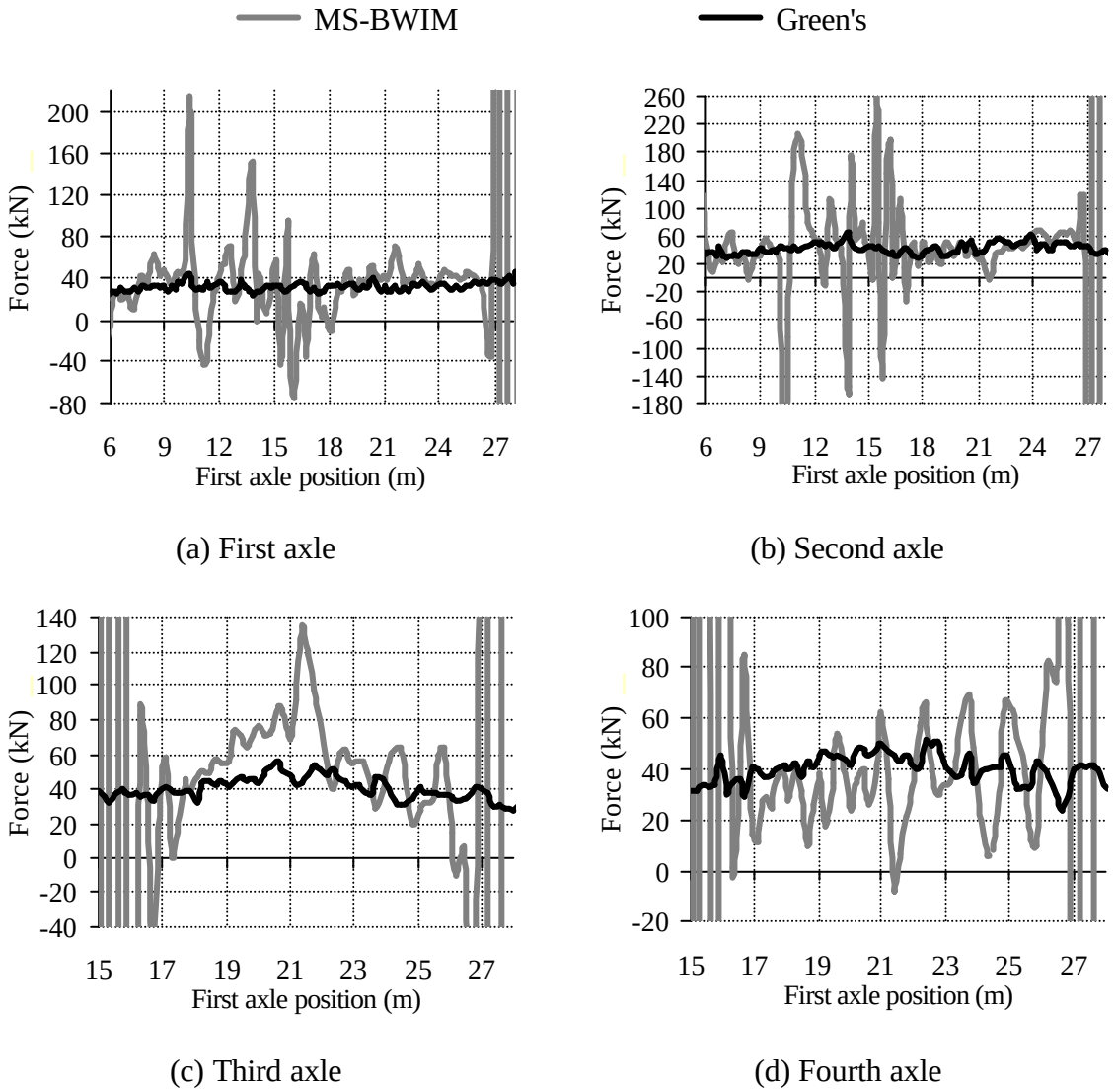

Figure 9.22 – Instantaneous calculation for a 4-axle truck (rough profile)

According to Tables 9.7, 9.8 and 9.9, gross weight is the only criterion which gives reasonable levels of accuracy. The static B-WIM gives the best result – C(15) for gross weight (Table 9.7). The other two algorithms are very inaccurate. However, if the test took

place in extended repeatability conditions (r2) taking into account only the runs of the air suspension truck, the accuracy class for gross weight would be raised to A(5), C(15) and C(15) for the static B-WIM, DB-WIM and MS-WIM algorithms respectively.

Table 9.7 – Accuracy classification for static B-WIM algorithm (beam model) (R1)

(**n**: Total number of vehicles; **m**: mean; **s**: Standard deviation; $\mathbf{p_0}$: level of confidence; **d**: tolerance of the retained accuracy class; $\mathbf{d_{min}}$: minimum width of the confidence interval for π_0; **p**: Level of confidence of the interval $[-\delta,\delta]$)

	Relative error statistics				Accuracy calculation				
Criterion	**n**	**m (%)**	**s (%)**	**p_0 (%)**	**Class**	**d (%)**	**d_{min} (%)**	**p (%)**	**Class Retained**
Single axle	36	-9.46	135.4	93.1	**E(300)**	360	300.4	97.3	**E(300)**
Group of axles	18	15.60	42.52	90.3	**E(100)**	110	100.1	93.6	
Gross Weight	18	0.95	5.71	90.3	**C(15)**	15	13.0	94.9	

Table 9.8 – Accuracy classification for DB-WIM algorithm (beam model) (R1)

(**n**: Total number of vehicles; **m**: mean; **s**: Standard deviation; $\mathbf{p_0}$: level of confidence; **d**: tolerance of the retained accuracy class; $\mathbf{d_{min}}$: minimum width of the confidence interval for π_0; **p**: Level of confidence of the interval $[-\delta,\delta]$)

	Relative error statistics				Accuracy calculation				
Criterion	**n**	**m (%)**	**s (%)**	**p_0 (%)**	**Class**	**d (%)**	**d_{min} (%)**	**p (%)**	**Class Retained**
Single axle	36	11.44	178.7	93.1	**E(395)**	474	396.0	97.3	**E(395)**
Group of axles	18	-15.59	55.86	90.3	**E(130)**	143	129.1	93.8	
Gross Weight	18	3.53	21.93	90.3	**E(50)**	50	49.8	90.4	

Table 9.9 – Accuracy classification for static MS-BWIM algorithm (beam model) (R1)

(**n**: Total number of vehicles; **m**: mean; **s**: Standard deviation; $\mathbf{p_0}$: level of confidence; **d**: tolerance of the retained accuracy class; $\mathbf{d_{min}}$: minimum width of the confidence interval for π_0; **p**: Level of confidence of the interval $[-\delta,\delta]$)

	Relative error statistics				Accuracy calculation				
Criterion	**n**	**m (%)**	**s (%)**	**p_0 (%)**	**Class**	**d (%)**	**d_{min} (%)**	**p (%)**	**Class Retained**
Single axle	36	-4.03	14.90	93.1	**E(30)**	36	33.9	94.8	**E(30)**
Group of axles	18	-4.89	21.42	90.3	**E(50)**	55	49.1	94.1	
Gross Weight	18	-4.07	12.13	90.3	**E(30)**	30	28.3	92.4	

Figure 9.23 illustrates the estimation of every identity in the sample.

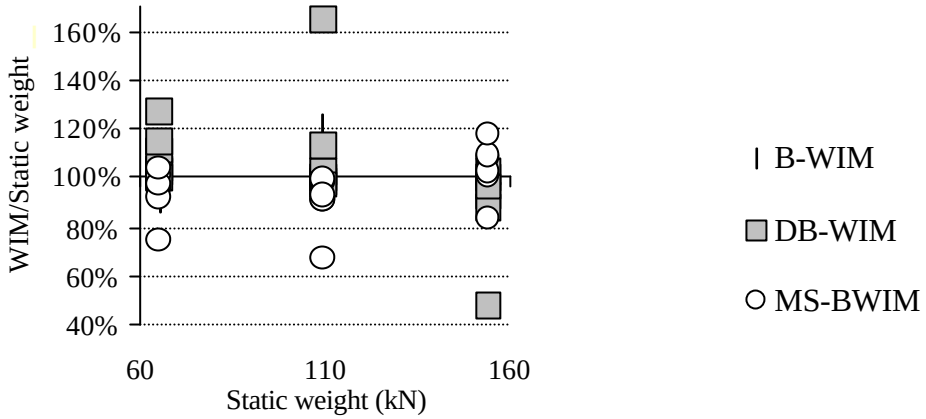

(a) Gross vehicle weight

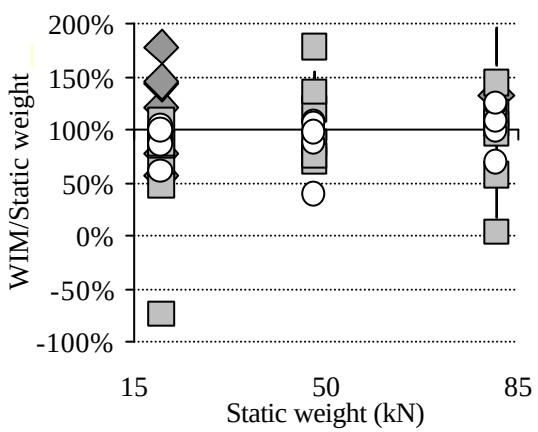

(b) Axle group

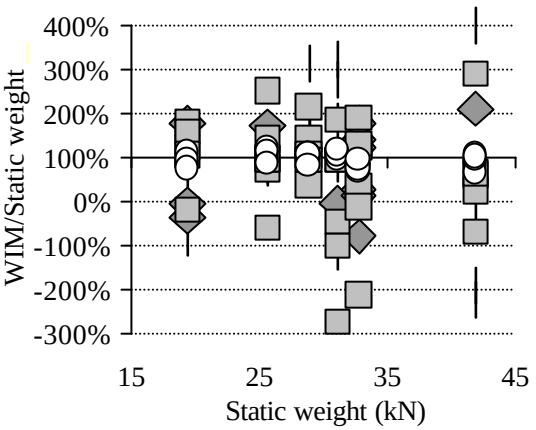

(c) Individual axle weights

Figure 9.23 – WIM/Static versus real static weights

9.3 TESTING WITH FINITE ELEMENT MODELS

Different types of bridge are used as the scenario for analysing the accuracy of each algorithm. The objective is analysing the influence of bridge dynamics on B-WIM accuracy for different B-WIM algorithms. It is hoped to achieve an improvement over the traditional static algorithm with the use of new locations and/or algorithms. Two and three-axle trucks with front axle and rear single axle or tandem are used in the tests. Individual axles of group spaced at 1.2 m. The redistribution of load between closely spaced axles is important, and the calculation of their individual weights is usually problematic. Truck

models are described in Section 6.4. The simulations take place under Limited Reproducibility conditions (R1).

The set of two vehicles are crossed over the bridge with three loading conditions at three different speed levels: 55, 70 and 85 km/h. The road surface roughness is generated from power spectral density functions based on the International Standards Organisation specifications for 'good' conditions. The characteristics of the simulations are given in Chapter 6.

The algorithms, based on strain from one longitudinal section, use sensors located at midspan unless otherwise specified. The positions of the sensors for the MS-BWIM approach are defined for each bridge. Strain is output every 0.004 s (250 Hz). The shape of the influence lines has been obtained from the models.

9.3.1 Isotropic Single Span Slab

Details of this 16 m bridge (First natural frequency 4.51 Hz) are given in Section 6.5.1. The traditional static B-WIM algorithm is tested with a different number of transverse locations at midspan: (a) 2 sensors at midspan (one in each lane at 2.5 m from the centreline) and (b) 8 sensors at midspan (spaced one metre apart along both lanes). The response of these sensors is added together before applying the algorithm. This sum is expected to compensate for torsional bending. Global accuracy remains C(15) regardless of the number of sensors at midspan (Tables 9.10 and 9.11).

Table 9.10 – Accuracy classification for static B-WIM (2 sensors) (Isotropic slab) (R1)

(**n**: Total number of vehicles; **m**: mean; **s**: Standard deviation; $\mathbf{p_0}$: level of confidence; **d**: tolerance of the retained accuracy class; $\mathbf{d_{min}}$: minimum width of the confidence interval for π_0; **p**: Level of confidence of the interval $[-\delta,\delta]$)

	Relative error statistics				Accuracy calculation				
Criterion	**n**	**m (%)**	**s (%)**	**p_o (%)**	**Class**	**d (%)**	**d_{min} (%)**	**p (%)**	**Class Retained**
Single axle	27	2.17	6.97	92.1	**C(15)**	20	16.1	97.5	**C(15)**
Group of axles	9	-2.20	2.73	83.4	**B+(7)**	10	7.3	96.2	
Gross Weight	18	0.01	0.95	90.3	**A(5)**	5	2.2	100.	

The results with a higher number of sensors are not more accurate (Table 9.11). In practice, B-WIM uses more than two sensors along one longitudinal section to overcome the limitations of the measurement devices (minimum detectable change in voltage, noise interference, etc.).

Table 9.11 – Accuracy classification for static B-WIM (8 sensors) (Isotropic slab) (R1)

(**n**: Total number of vehicles; **m**: mean; **s**: Standard deviation; $\mathbf{p_0}$: level of confidence; **d**: tolerance of the retained accuracy class; $\mathbf{d_{min}}$: minimum width of the confidence interval for π_0; **p**: Level of confidence of the interval $[-\delta,\delta]$)

	Relative error statistics				Accuracy calculation				
Criterion	**n**	**m (%)**	**s (%)**	**p_0 (%)**	**Class**	**d (%)**	**d_{min} (%)**	**p (%)**	**Class Retained**
Single axle	27	2.16	6.97	92.1	**C(15)**	20	16.1	97.5	**C(15)**
Group of axles	9	-2.22	2.74	83.4	**B+(7)**	10	7.3	96.1	
Gross Weight	18	0.01	0.98	90.3	**A(5)**	5	2.2	100.	

Table 9.12 shows results for the dynamic algorithm based on one longitudinal section. Overall accuracy decreases to D+(20). There is a slight improvement in accuracy for gross weight, but the use of the dynamic algorithm is not justifiable for this particular bridge.

Table 9.12 – Accuracy classification for DB-WIM algorithm (Isotropic slab) (R1)

(**n**: Total number of vehicles; **m**: mean; **s**: Standard deviation; $\mathbf{p_0}$: level of confidence; **d**: tolerance of the retained accuracy class; $\mathbf{d_{min}}$: minimum width of the confidence interval for π_0; **p**: Level of confidence of the interval $[-\delta,\delta]$)

	Relative error statistics				Accuracy calculation				
Criterion	**n**	**m (%)**	**s (%)**	**p_0 (%)**	**Class**	**d (%)**	**d_{min} (%)**	**p (%)**	**Class Retained**
Single axle	27	3.50	8.97	92.1	**D+(20)**	25	21.1	96.7	**D+(20)**
Group of axles	9	-3.61	3.80	83.4	**B(10)**	13	10.6	93.3	
Gross Weight	18	0.00	0.80	90.3	**A(5)**	5	1.8	100.	

The B-WIM static algorithm is more accurate because it generates a hypothetical static response closer to the static strain than the DB-WIM curve is to the total strain. The approximation by DB-WIM of the runs for the heaviest three-axle truck at 55 and 85 km/h is shown in Figures 9.24(a) and (b) respectively. Bridge vibrations in the tail of the strain record are not properly matched at highest speeds. The source of this inaccuracy is the non-

linear nature of the dynamic problem. DB-WIM is unaware of the initial conditions of displacement, velocity and acceleration of the bridge, which induces a deviation in the matching, particularly significant when the first axle leaves the bridge.

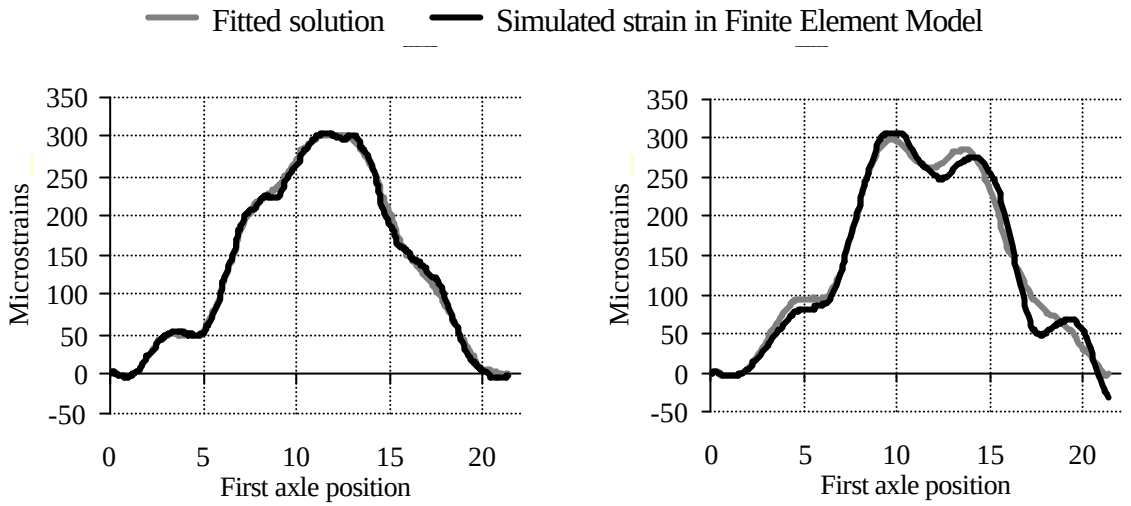

(a) Three-axle truck at 55 km/h (b) Three-axle truck at 85 km/h

Figure 9.24 – Approximation by the static and dynamic Algorithms

If the DB-WIM is applied purely to the strain record before the first axle leaves the bridge, accuracy should improve. Results are shown in Table 9.13. Overall accuracy increases to C(15), but the static approach still offers a slightly better solution.

Table 9.13 – Accuracy classification for DB-WIM (shorter record) (Isotropic slab) (R1)

(**n**: Total number of vehicles; **m**: mean; **s**: Standard deviation; $\mathbf{p_0}$: level of confidence; **d**: tolerance of the retained accuracy class; $\mathbf{d_{min}}$: minimum width of the confidence interval for π_0; **p**: Level of confidence of the interval $[-\delta,\delta]$)

	Relative error statistics				Accuracy calculation				
Criterion	**n**	**m (%)**	**s (%)**	**p_0 (%)**	**Class**	**d (%)**	**d_{min} (%)**	**p (%)**	**Class Retained**
Single axle	27	2.99	8.33	92.1	**C(15)**	20	19.4	93.1	**C(15)**
Group of axles	9	-2.96	2.43	83.4	**B+(7)**	10	7.4	96.6	
Gross Weight	18	0.02	1.39	90.3	**A(5)**	5	3.1	99.4	

Hence, it can be concluded that DB-WIM is not valid in situations where the bridge has been previously excited (i.e. initial state of vibration due to the passing of a preceding truck). Accordingly, DB-WIM should not be applied to very short span bridges.

The MS-BWIM system was tested with strain at three longitudinal sections (4, 8 and 12 m) and two transverse positions per section (under the slow and fast lane at 2.5 m from the centreline). Six static equations can be formulated at each instant (one per sensor), but the algorithm is not able to predict an instantaneous solution at all times. There are instants where numerical errors appear and they should be removed from the calculations. The determinant has very small values when there is a change in the number of axles on the bridge. Thus, for the 2-axle truck with 5 m axle spacing, the instantaneous solution will tend towards infinity at 5 m and 16 m (the contribution of an axle entering or leaving the bridge to the overall strain is negligible). As the number of axles increases, the length of the bridge where the instantaneous calculation is feasible decreases as does the accuracy. Accuracy classes for this choice of sensors are given in Table 9.14. Compared to the algorithms based on one longitudinal location, there is an improvement from C(15) to A(5). Therefore, if the criterion for an axle of group is considered, overall accuracy D+(20) is achieved (accuracy by algorithms based on one longitudinal location for axle of a group is very poor). However, as the COST323 specification does not require axles of groups for B-WIM systems, the system is strictly of class A(5).

Table 9.14 – Accuracy classification for static MS-BWIM (3 longit. sections) (slab) (R1)

(**n**: Total number of vehicles; **m**: mean; **s**: Standard deviation; $\mathbf{p_0}$: level of confidence; **d**: tolerance of the retained accuracy class; $\mathbf{d_{min}}$: minimum width of the confidence interval for π_0; **p**: Level of confidence of the interval $[-\delta,\delta]$)

	Relative error statistics				**Accuracy calculation**				
Criterion	**n**	**m (%)**	**S (%)**	**p_o (%)**	**Class**	**d (%)**	**d_{min} (%)**	**p (%)**	**Class Retained**
Single axle	27	-1.15	2.73	92.1	**A(5)**	8	6.5	97.5	**D+(20)**
Axle of group	18	-1.07	12.34	90.3	**D+(20)**	30	27.9	92.9	
Group of axles	9	1.01	1.52	83.4	**A(5)**	7.14	3.9	99.3	
Gross Weight	18	0.01	0.83	90.3	**A(5)**	5	1.9	100.	

The number and location of the sensors have a strong influence on the duration for which the instantaneous solution is possible. Next, the MS-BWIM system is tested with sensors located every 2 m all along the bridge. Two transverse sensors under the slow and fast lanes are considered for each longitudinal section (Their results are added together). This results in 7 static equations solved by a least squares fitting technique as described in Section 7.5.2. The instantaneous solution is feasible for longer and the final average value

should be closer to the static weight. This time, the overall accuracy is B+(7), or A(5) excluding the axle of group criterion (Table 9.15). This MS-BWIM system offers a very significant improvement over all previous approaches. The increase in the number of instrumented sections from 3 to 7 has raised accuracy for axles of group from D+(20) to B+(7).

Table 9.15 – Accuracy classification for static MS-BWIM (7 longit. sections) (slab) (R1)

(**n**: Total number of vehicles; **m**: mean; **s**: Standard deviation; $\mathbf{p_0}$: level of confidence; **d**: tolerance of the retained accuracy class; $\mathbf{d_{min}}$: minimum width of the confidence interval for π_0; **p**: Level of confidence of the interval $[-\delta,\delta]$)

	Relative error statistics				Accuracy calculation				
Criterion	**n**	**m (%)**	**S (%)**	**p_0 (%)**	**Class**	**d (%)**	**d_{min} (%)**	**p (%)**	**Class Retained**
Single axle	27	-0.45	1.39	92.1	**A(5)**	8	3.2	100.	**B+(7)**
Axle of group	18	0.88	4.42	90.3	**B+(7)**	14	10.1	98.2	
Group of axles	9	0.57	0.54	83.4	**A(5)**	7.14	1.6	100.	
Gross Weight	18	0.00	0.64	90.3	**A(5)**	5	1.5	100.	

Figure 9.25 shows the results achieved by the different algorithms.

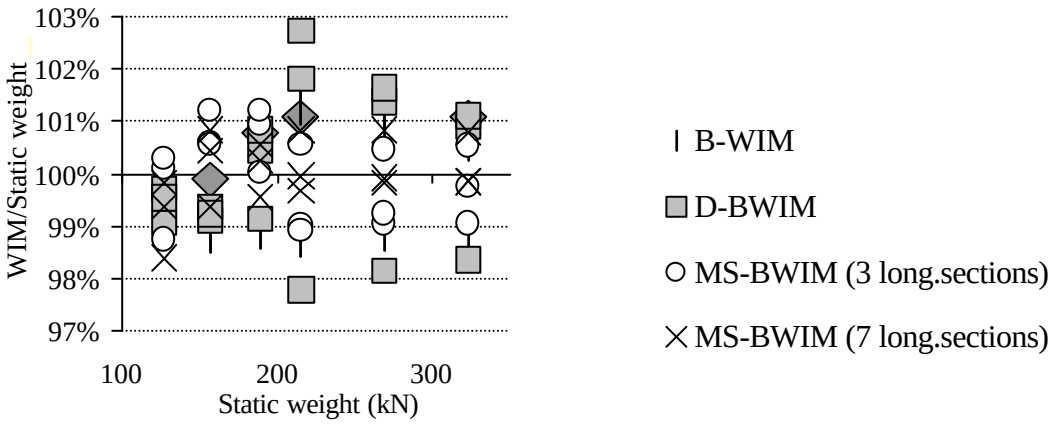

(a) Gross vehicle weight

Figure 9.25 (continued on following page)

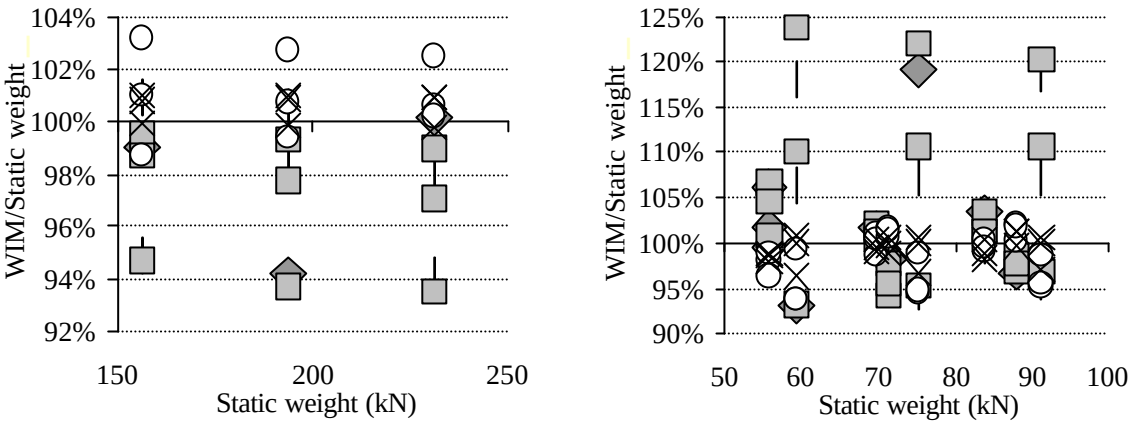

(b) Axle group (c) Individual axle weights

Figure 9.25 – WIM/Static versus real static weights (Isotropic slab)

The previous results for MS-BWIM were obtained by averaging the instantaneous values for each axle. However, the potential of an instantaneous calculation can be further exploited. If the dynamic oscillation of the predicted load is considered, accuracy could be expected to improve (i.e., avoiding deviations that depend on the time the truck is on the bridge). The dominant frequency of higher amplitude can be obtained through the spectra of the varying axle load amplitude (generally corresponding to the first natural frequency of the bridge, but it could be another frequency resulting from the bridge-truck interaction). Then, the static value can be obtained through the average of an exact number of periods. The same process can be used to remove remaining frequency components. If the lower frequency components can not be detected by the spectra (i.e. readings that do not complete a period), the parameters of the harmonic oscillation (amplitude, frequency and phase) can be adjusted to the available data. Figure 9.26(a) represents the original history of axle forces obtained by MS-BWIM. Figures 9.26(b) and 9.26(c) show the removal of frequency components in successive steps. Averaging the values in Figure 9.26(c) results in 52.9 and 68.5 kN, slightly smaller than the real static axle weights of 55.7 and 71.2 kN respectively. The final static value can be derived from Figure 9.26(c) by applying trigonometry to the remaining low frequency component. This technique can be of great interest in bridges where the number of dynamic oscillations is not high enough.

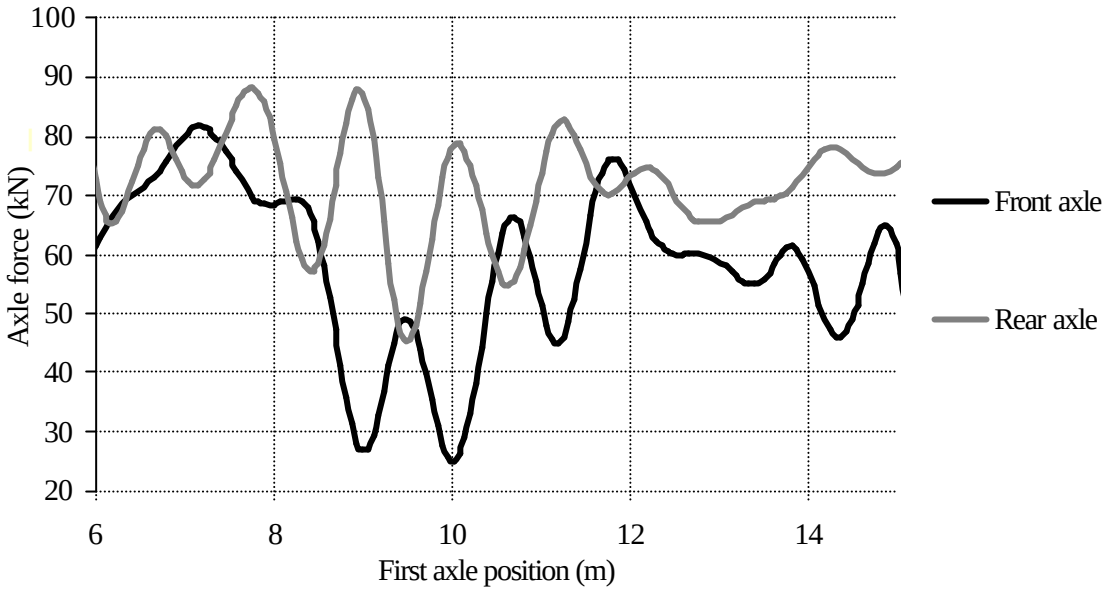

(a) Initial Prediction of Instantaneous axle forces

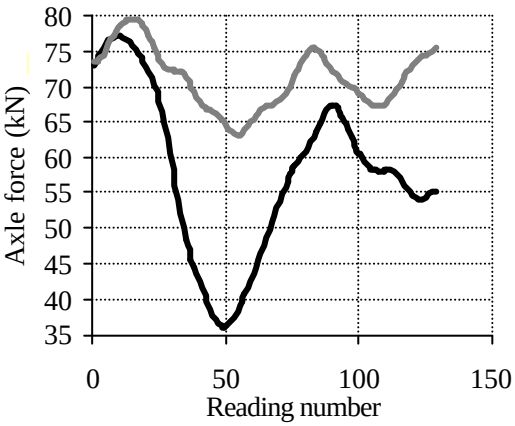

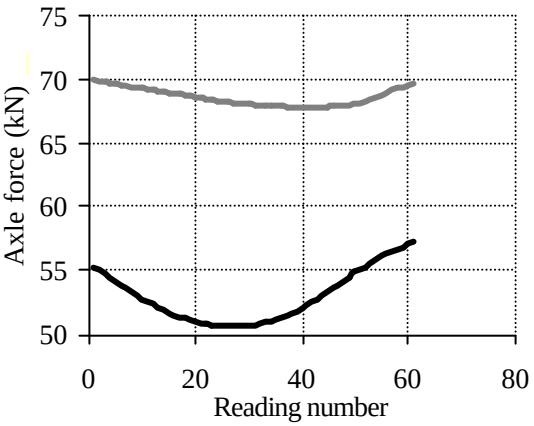

(b) Removal of 13.16 Hz frequency (c) Removal of 3.62 Hz frequency

Figure 9.26 – Estimation of static value (fully laden two-axle truck at 55 km/h)

Effect of truck lateral location

All previous runs were located in the same lateral path (inner wheels at 1 m from the bridge centreline). In this section, new runs with small variations in the lateral position on the road are included in the accuracy analysis. The inner wheels of the truck are in the slow lane at 0, 1 and 2 m from the bridge centreline (Figure 6.40). The prediction in weights by the static algorithm is shown in Figure 9.27.

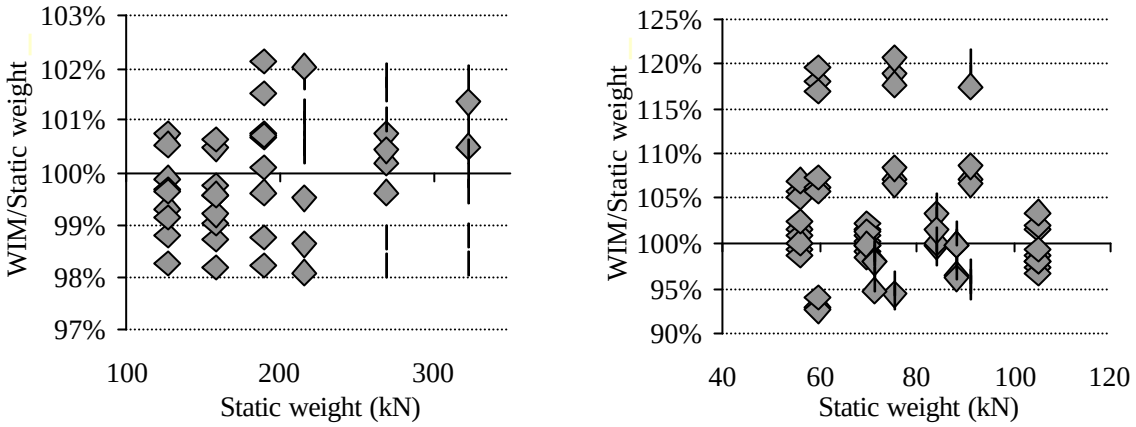

(a) Gross vehicle weight (b) Individual axle weights

Figure 9.27 – WIM/Static versus real static weights

The static algorithm maintains the same accuracy classes as Table 9.10 (one lateral position) for each individual criterion (Table 9.16). Accuracy of individual axle weight results are more robust (higher confidence interval) as a result of a bigger sample.

Table 9.16 – Accuracy classification for static B-WIM (2 sensors) (Isotropic slab) (R1)

(**n**: Total number of vehicles; **m**: mean; **s**: Standard deviation; $\mathbf{p_0}$: level of confidence; **d**: tolerance of the retained accuracy class; $\mathbf{d_{min}}$: minimum width of the confidence interval for π_0; **p**: Level of confidence of the interval $[-\delta,\delta]$)

	Relative error statistics				**Accuracy calculation**				
Criterion	**n**	**m (%)**	**s (%)**	**p_0 (%)**	**Class**	**d (%)**	**d_{min} (%)**	**p (%)**	**Class Retained**
Single axle	81	2.21	6.93	94.6	C(15)	20	15.77	98.7	**C(15)**
Group of axles	27	-2.26	2.67	92.1	B+(7)	10	7.25	99.0	
Gross Weight	54	0.01	1.12	94.0	A(5)	5	2.46	99.9	

In this case, the transverse location of the truck does not affect accuracy. However, a two-dimensional algorithm as proposed in Section 7.6 can improve results in bridges sensitive to the transverse location. This algorithm is based on a database of influence lines for each truck transverse location. The correct influence line can be chosen at each instant by minimising errors between measured and theoretical strains (instead of using a common influence line as with one-dimensional models).

9.3.2 Two-Span Isotropic Slab

Details of this 37-m bridge (First natural frequency 4.18 Hz) are given in Section 6.5.2. The static B-WIM system uses strain at the middle of the first span (at two points symmetric about the centreline and spaced 5 m transversely). Table 9.17 shows how a global accuracy of D+(20) is achieved. Compared to the single span studied in the previous section, the algorithm is less accurate in this longer bridge due to the difficulty of weighing single axles and the higher dynamics at the midspan section. Accuracy in GVW and axle groups remains at A(5) and B+(7) respectively.

The same sensors are used to test the dynamic B-WIM algorithm. Results are shown in Table 9.18. Accuracy in single axles improves from D+(20) to B(10). However, if the criterion of axle of group is considered, the overall accuracy decreases down to E(60).

Table 9.17 – Accuracy classification for static B-WIM (midspan) (Two-span slab) (R1)

(**n**: Total number of vehicles; **m**: mean; **s**: Standard deviation; $\mathbf{p_0}$: level of confidence; **d**: tolerance of the retained accuracy class; $\mathbf{d_{min}}$: minimum width of the confidence interval for π_0; **p**: Level of confidence of the interval $[-\delta,\delta]$)

	Relative error statistics				Accuracy calculation				
Criterion	**n**	**m (%)**	**s (%)**	**p_0 (%)**	**Class**	**d (%)**	**d_{min} (%)**	**p (%)**	**Class Retained**
Single axle	27	1.71	9.67	92.1	**D+(20)**	25	21.8	96.0	**D+(20)**
Group of axles	9	-1.56	3.91	83.4	**B+(7)**	10	9.4	86.9	
Gross Weight	18	0.02	1.39	90.3	**A(5)**	5	3.1	99.4	

Table 9.18 – Accuracy classification for DB-WIM algorithm (Two-span slab) (R1)

(**n**: Total number of vehicles; **m**: mean; **s**: Standard deviation; $\mathbf{p_0}$: level of confidence; **d**: tolerance of the retained accuracy class; $\mathbf{d_{min}}$: minimum width of the confidence interval for π_0; **p**: Level of confidence of the interval $[-\delta,\delta]$)

	Relative error statistics				Accuracy calculation				
Criterion	**n**	**m (%)**	**s (%)**	**p_0 (%)**	**Class**	**d (%)**	**d_{min} (%)**	**p (%)**	**Class Retained**
Single axle	27	1.97	5.85	92.1	**B(10)**	15	13.6	95.1	**E(60)**
Axle of group	18	1.82	29.13	90.3	**E(60)**	77	65.7	95.3	
Group of axles	9	-1.88	2.15	83.4	**A(5)**	7.14	5.9	92.9	
Gross Weight	18	0.00	0.63	90.3	**A(5)**	5	1.4	100.	

The central support is expected to suffer less dynamic vibrations, and a static B-WIM system based on this location is also tested. Table 9.19 shows an improvement in single axle weights from B(10) to A(5), and in axle of a group from E(60) to B(+7). The system is extraordinarily accurate, even for individual axles in a group. Global accuracy is B+(7). The most accurate class, A(5), is reached if the criterion of axle of group is ignored.

Table 9.19 – Accuracy classification for static B-WIM (central support) (Two-span slab)

(**n**: Total number of vehicles; **m**: mean; **s**: Standard deviation; $\mathbf{p_0}$: level of confidence; **d**: tolerance of the retained accuracy class; $\mathbf{d_{min}}$: minimum width of the confidence interval for π_0; **p**: Level of confidence of the interval $[-\delta,\delta]$)

	Relative error statistics				**Accuracy calculation**				
Criterion	**n**	**m (%)**	**s (%)**	**p_o (%)**	**Class**	**d (%)**	**d_{min} (%)**	**p (%)**	**Class Retained**
Single axle	27	-0.25	2.45	92.1	**A(5)**	8	5.5	99.2	**B+(7)**
Axle of group	18	-0.18	5.54	90.3	**B+(7)**	14	12.5	94.1	
Group of axles	9	0.45	0.58	83.4	**A(5)**	7.14	1.5	100.	
Gross Weight	18	0.00	0.56	90.3	**A(5)**	5	1.3	100.	

The MS-BWIM system use strains at 5.9, 9.5, 11.9, 17.9, 23.9, 27.5 and 29.9 m from the bridge start in two transverse positions (under the slow and fast lanes at 2.5 m from the centreline). A global accuracy of B(10) is obtained in Table 9.20. The best option appears to be the static algorithm purely based on the instrumentation of the central support section. The consideration of other less accurate longitudinal locations in an instantaneous calculation results in a lower accuracy class.

Table 9.20 – Accuracy classification for static MS-BWIM (Two-span isotropic slab) (R1)

(**n**: Total number of vehicles; **m**: mean; **s**: Standard deviation; $\mathbf{p_0}$: level of confidence; **d**: tolerance of the retained accuracy class; $\mathbf{d_{min}}$: minimum width of the confidence interval for π_0; **p**: Level of confidence of the interval $[-\delta,\delta]$)

	Relative error statistics				**Accuracy calculation**				
Criterion	**n**	**m (%)**	**s (%)**	**p_o (%)**	**Class**	**d (%)**	**d_{min} (%)**	**p (%)**	**Class Retained**
Single axle	27	1.16	3.00	92.1	**A(5)**	8	7.1	95.8	**B(10)**
Axle of group	18	-1.22	7.17	90.3	**B(10)**	20	16.3	96.3	
Group of axles	9	-1.43	1.31	83.4	**A(5)**	7.14	3.8	99.6	
Gross Weight	18	0.01	1.18	90.3	**A(5)**	5	2.7	99.8	

Finally, Figure 9.28 shows the performance of each algorithm in the estimation of gross vehicle weight, axle group and single axle.

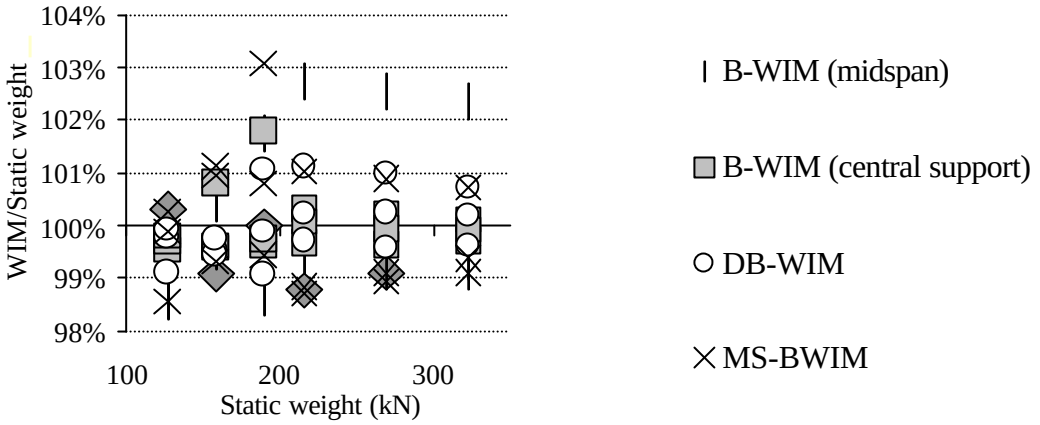

(a) Gross vehicle weight

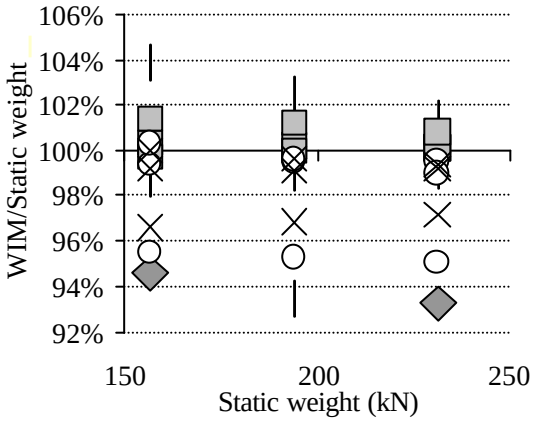

(b) Axle group

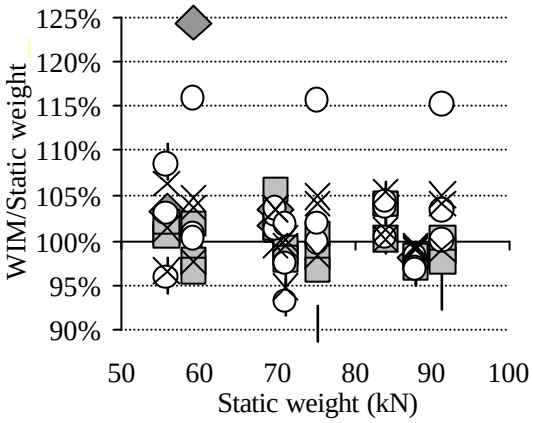

(c) Individual axle weights

Figure 9.28 – WIM/Static versus real static weights (Two-span isotropic slab)

9.3.3 Slab with Edge Cantilever

Details of this 20 m bridge (First natural frequency 4.80 Hz) are given in Section 6.5.3. The results of the static algorithm are based on strains by two sensors located at the midspan section. This bridge is stiffer than the single span isotropic slab in Section 9.3.1. This bridge has also a longer span with a higher first natural frequency. Bridge dynamics are expected to be smaller and the average of the varying axle forces closer to the static value. Accuracy should improve with respect to the global accuracy C(15) obtained in the single span isotropic slab. Consistently, Table 9.21 shows an accuracy of B(10) when ignoring the criterion of axle of group. This last criterion has a very poor accuracy E(70).

Table 9.21 – Accuracy classification for static B-WIM (Slab with edge cantilever) (R1)

(**n**: Total number of vehicles; **m**: mean; **s**: Standard deviation; $\mathbf{p_0}$: level of confidence; **d**: tolerance of the retained accuracy class; $\mathbf{d_{min}}$: minimum width of the confidence interval for π_0; **p**: Level of confidence of the interval $[-\delta,\delta]$)

	Relative error statistics				Accuracy calculation				
Criterion	**n**	**m (%)**	**s (%)**	**p_o (%)**	**Class**	**d (%)**	**d_{min} (%)**	**p (%)**	**Class Retained**
Single axle	27	0.73	5.64	92.1	**B(10)**	15	12.6	96.7	**E(70)**
Axle of group	18	1.80	33.54	90.3	**E(70)**	89	75.6	95.4	
Group of axles	9	-0.53	2.25	83.4	**A(5)**	7.14	5.2	95.4	
Gross Weight	18	0.01	0.80	90.3	**A(5)**	5	1.8	100.	

Table 9.22 gives accuracy classes when applying a dynamic B-WIM to the same sensors. The dynamic approach is less accurate and unsuitable for this type of bridge behaviour.

Table 9.22 – Accuracy classification for DB-WIM (Slab with edge cantilever) (R1)

(**n**: Total number of vehicles; **m**: mean; **s**: Standard deviation; $\mathbf{p_0}$: level of confidence; **d**: tolerance of the retained accuracy class; $\mathbf{d_{min}}$: minimum width of the confidence interval for π_0; **p**: Level of confidence of the interval $[-\delta,\delta]$)

	Relative error statistics				Accuracy calculation				
Criterion	**n**	**m (%)**	**s (%)**	**p_o (%)**	**Class**	**d (%)**	**d_{min} (%)**	**p (%)**	**Class Retained**
Single axle	27	1.54	6.88	92.1	**C(15)**	20	15.6	97.9	**E(90)**
Axle of group	18	2.21	42.26	90.3	**E(90)**	113	95.3	95.6	
Group of axles	9	-1.38	2.81	83.4	**A(5)**	7.14	6.9	85.5	
Gross Weight	18	0.00	0.72	90.3	**A(5)**	5	1.6	100.	

MS-BWIM uses strain in six different points at 4.5, 9.5 and 14.5 m from the bridge start in two transverse positions (under the slow and fast lane at 2.5 m from the centreline). MS-BWIM offers the most accurate overall class A(5) (Table 9.23).

Figure 9.29(c) illustrates how MS-BWIM is the best solution for individual axles. However, B-WIM is lightly more reliable when estimating axle group or gross weight (Figures 9.29(a) and (b)).

Table 9.23 – Accuracy classification for static MS-BWIM (Slab with edge cantilever) (R1)

(**n**: Total number of vehicles; **m**: mean; **s**: Standard deviation; $\mathbf{p_0}$: level of confidence; **d**: tolerance of the retained accuracy class; $\mathbf{d_{min}}$: minimum width of the confidence interval for π_0; **p**: Level of confidence of the interval $[-\delta,\delta]$)

	Relative error statistics				Accuracy calculation				
Criterion	**n**	**m (%)**	**s (%)**	**p_o (%)**	**Class**	**d (%)**	**d_{min} (%)**	**p (%)**	**Class Retained**
Single axle	27	0.76	3.40	92.1	**A(5)**	8	7.7	93.4	**A(5)**
Axle of group	18	-0.50	3.42	90.3	**A(5)**	10	7.8	97.2	
Group of axles	9	-0.53	1.81	83.4	**A(5)**	7.14	4.3	98.5	
Gross Weight	18	0.03	1.92	90.3	**A(5)**	5	4.3	95.0	

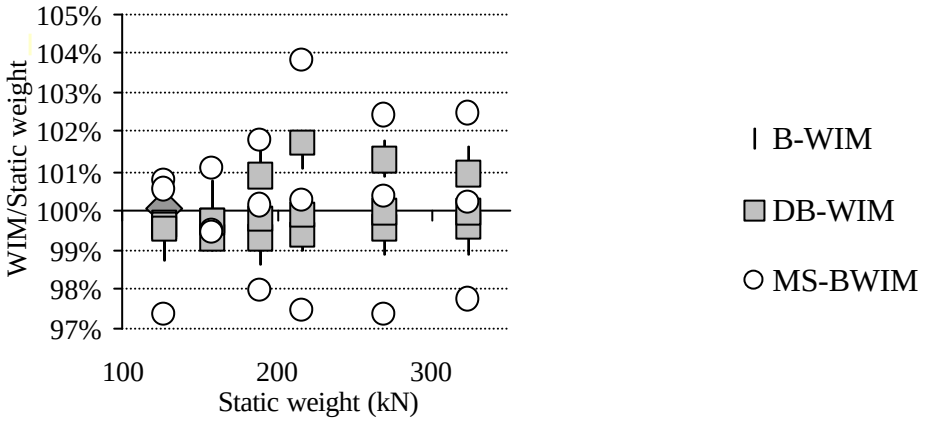

(a) Gross vehicle weight

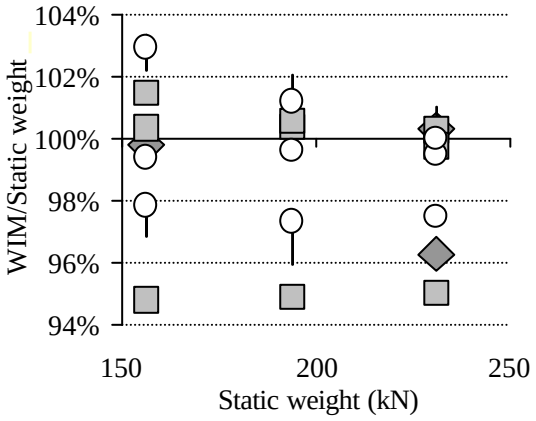

(b) Axle group

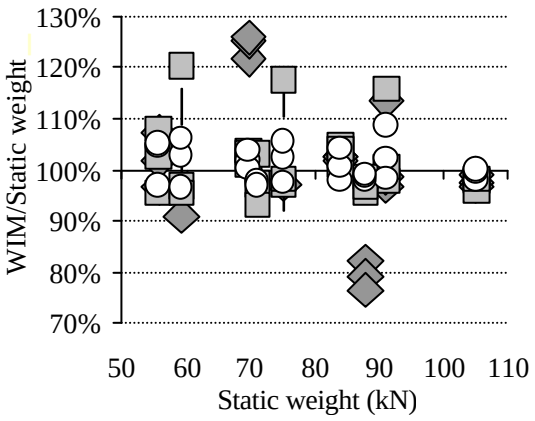

(c) Individual axle weights

Figure 9.29 – WIM/Static versus real static weights (Slab with edge cantilever)

9.3.4 Voided Slab Deck

Details of this 25 m bridge (First natural frequency 3.80 Hz) are given in Section 6.5.4. The static B-WIM algorithm uses two sensors at midspan (one sensor in each lane at 2.5 m from centreline). This bridge is longer and more flexible than the previous slab with edge cantilever. Thus, poorer results are expected, particularly for single axle weights. Table 9.24 shows how the overall accuracy class comes down to D(25).

Table 9.24 – Accuracy classification for static B-WIM algorithm (Voided Slab) (R1)

(**n**: Total number of vehicles; **m**: mean; **s**: Standard deviation; $\mathbf{p_0}$: level of confidence; **d**: tolerance of the retained accuracy class; $\mathbf{d_{min}}$: minimum width of the confidence interval for π_0; **p**: Level of confidence of the interval $[-\delta,\delta]$)

	Relative error statistics				Accuracy calculation				
Criterion	**n**	**m (%)**	**s (%)**	**p_0 (%)**	**Class**	**d (%)**	**d_{min} (%)**	**p (%)**	**Class Retained**
Single axle	27	-3.47	12.00	92.1	**D(25)**	30	27.6	94.7	**D(25)**
Group of axles	9	3.96	6.56	83.4	**C(15)**	18	16.5	88.0	
Gross Weight	18	0.00	0.48	90.3	**A(5)**	5	1.1	100.	

The dynamic algorithm is tested with the same sensors and accuracy improves from D(25) to C(15) (Table 9.25).

Table 9.25 – Accuracy classification for dynamic B-WIM algorithm (Voided Slab) (R1)

(**n**: Total number of vehicles; **m**: mean; **s**: Standard deviation; $\mathbf{p_0}$: level of confidence; **d**: tolerance of the retained accuracy class; $\mathbf{d_{min}}$: minimum width of the confidence interval for π_0; **p**: Level of confidence of the interval $[-\delta,\delta]$)

	Relative error statistics				Accuracy calculation				
Criterion	**n**	**m (%)**	**s (%)**	**p_0 (%)**	**Class**	**d (%)**	**d_{min} (%)**	**p (%)**	**Class Retained**
Single axle	27	2.74	8.38	92.1	**C(15)**	20	19.4	93.2	**C(15)**
Group of axles	9	-2.75	3.83	83.4	**B+(7)**	10	10.0	83.6	
Gross Weight	18	0.00	0.72	90.3	**A(5)**	5	1.6	100.	

The MS-BWIM system use strain in six different points at 6.5, 12.5 and 18.5 m from the bridge start in two transverse positions (under the slow and fast lane at 2.5 m from the centreline). As shown in Table 9.26, MS-BWIM is more inaccurate for gross weight and

axle group than algorithms based on one longitudinal section. The cause is the reduced number and inappropriate location of sensors that only allow for an instantaneous solution for a short period of time (along one meter for the tandem at highest speed). Compared to the previous slab with edge cantilever, this is a longer bridge that requires more sensors to cover most of the vehicle path effectively. Therefore, static equations are not a good reference for the behaviour of this bridge as accuracy in Table 9.24 reveals.

Table 9.26 – Accuracy classification for static MS-BWIM algorithm (Voided Slab) (R1)

(**n**: Total number of vehicles; **m**: mean; **s**: Standard deviation; $\mathbf{p_0}$: level of confidence; **d**: tolerance of the retained accuracy class; $\mathbf{d_{min}}$: minimum width of the confidence interval for π_0; **p**: Level of confidence of the interval $[-\delta,\delta]$)

	Relative error statistics				Accuracy calculation				
Criterion	**n**	**m (%)**	**s (%)**	**p_o (%)**	**Class**	**d (%)**	**d_{min} (%)**	**p (%)**	**Class Retained**
Single axle	27	-2.65	6.71	92.1	C(15)	20	15.8	97.8	**D+(20)**
Group of axles	9	4.99	7.03	83.4	D+(20)	23	18.2	93.9	
Gross Weight	18	0.27	5.58	90.3	C(15)	15	12.6	95.7	

Figure 9.30 illustrates the accuracy for different approaches. Percentage errors in individual axle weights generally increase for higher speeds and lower weights (Figure 9.30(c)).

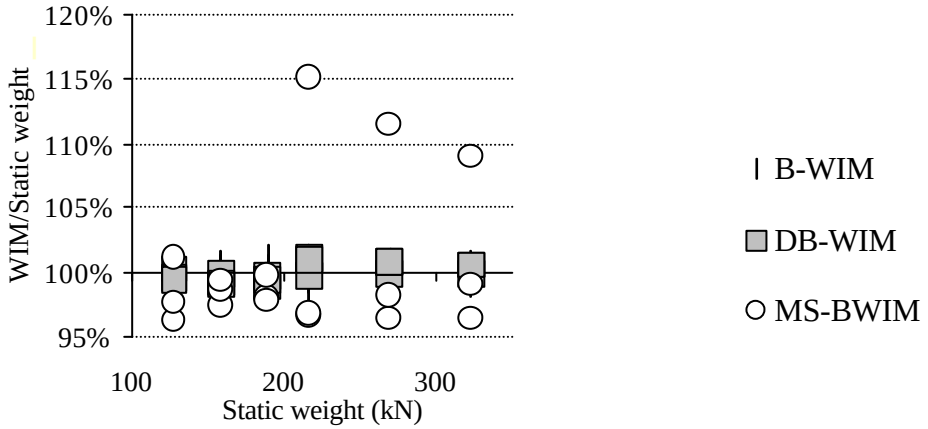

(a) Gross vehicle weight

Figure 30 (continued on following page)

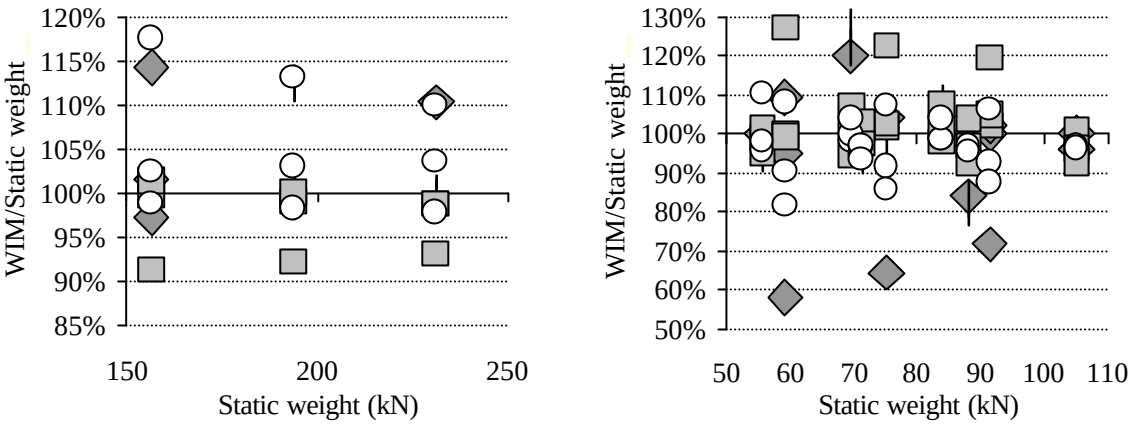

(b) Axle group (c) Individual axle weights

Figure 9.30 – WIM/Static versus real static weights (Voided slab deck)

9.3.5 Beam and Slab

Details of this 20 m bridge (first natural frequency 6.13 Hz) are given in Section 6.5.5. This bridge has the same length, less stiffness (higher static strain) and higher first natural frequency than the slab with edge cantilever. At the midspan section, transverse bending of the slab is more significant than longitudinal bending. In preceding sections, the magnitude of this transverse bending was too small to be considered. Unlike longitudinal bending, the influence line for transverse bending has opposite curvature under the slow and fast lanes. The algorithms based on one longitudinal location use two sensors at the midspan section. Three different possibilities are studied:

(a) use of the beam longitudinal strain (sum of two sensors 3 m apart, located symmetrically about the centreline) (accuracy analysis in Table 9.27),
(b) use of the slab longitudinal bending (sum of two sensors 4 m apart, located symmetrically about the centreline) (Table 9.28), and
(c) use of the slab transverse bending (difference of two sensors 4 m apart, located symmetrically about the centreline) (Table 9.29).

If the axle of a group criterion is included in the analysis, a best overall result of B+(7) is obtained with installation (c), compared to D(25) and E(30) for options (a) and (b) respectively. If axle of group is ignored in the analysis, overall accuracy raises to A(5) when using transverse strain and B+(7) for longitudinal bending. Hence, though B-WIM

systems have always used longitudinal bending for weighing purposes, the measurement of transverse bending must require further attention for particular sites.

Table 9.27 – Accuracy classification for static B-WIM (beam) (Beam&Slab bridge) (R1)

(**n**: Total number of vehicles; **m**: mean; **s**: Standard deviation; $\mathbf{p_0}$: level of confidence; **d**: tolerance of the retained accuracy class; $\mathbf{d_{min}}$: minimum width of the confidence interval for π_0; **p**: Level of confidence of the interval $[-\delta,\delta]$)

	Relative error statistics				Accuracy calculation				
Criterion	**n**	**m (%)**	**s (%)**	**p_o (%)**	**Class**	**d (%)**	**d_{min} (%)**	**p (%)**	**Class Retained**
Single axle	27	-1.13	3.96	92.1	**B+(7)**	11	9.1	96.9	**D(25)**
Axle of group	18	-0.96	14.89	90.3	**D(25)**	35	33.6	91.8	
Group of axles	9	1.39	1.64	83.4	**A(5)**	7.14	4.4	98.6	
Gross Weight	18	0.00	0.50	90.3	**A(5)**	5	1.1	100.	

Table 9.28 – Accuracy classification for static B-WIM (slab longitud. strain) (B&S) (R1)

(**n**: Total number of vehicles; **m**: mean; **s**: Standard deviation; $\mathbf{p_0}$: level of confidence; **d**: tolerance of the retained accuracy class; $\mathbf{d_{min}}$: minimum width of the confidence interval for π_0; **p**: Level of confidence of the interval $[-\delta,\delta]$)

	Relative error statistics				Accuracy calculation				
Criterion	**n**	**m (%)**	**s (%)**	**p_o (%)**	**Class**	**d (%)**	**d_{min} (%)**	**p (%)**	**Class Retained**
Single axle	27	-0.57	4.29	92.1	**B+(7)**	11	9.6	95.8	**E(30)**
Axle of group	18	-0.37	15.87	90.3	**E(30)**	41	35.7	94.8	
Group of axles	9	0.85	1.61	83.4	**A(5)**	7.14	4.0	99.2	
Gross Weight	18	0.00	0.46	90.3	**A(5)**	5	1.0	100.	

Table 9.29 – Accuracy classification for static B-WIM (slab transvers. strain) (B&S) (R1)

(**n**: Total number of vehicles; **m**: mean; **s**: Standard deviation; $\mathbf{p_0}$: level of confidence; **d**: tolerance of the retained accuracy class; $\mathbf{d_{min}}$: minimum width of confidence interval for π_0; **p**: Level of confidence of $[-\delta,\delta]$)

	Relative error statistics				Accuracy calculation				
Criterion	**n**	**m (%)**	**s (%)**	**p_o (%)**	**Class**	**d (%)**	**d_{min} (%)**	**p (%)**	**Class Retained**
Single axle	27	0.50	2.07	92.1	**A(5)**	8	4.7	99.8	**B+(7)**
Axle of group	18	-0.09	5.39	90.3	**B+(7)**	14	12.1	94.9	
Group of axles	9	-0.45	0.52	83.4	**A(5)**	7.14	1.4	100.	
Gross Weight	18	0.00	0.30	90.3	**A(5)**	5	0.7	100.	

The dynamic algorithm is applied to the longitudinal bending of two beams at midspan. Results, given in Table 9.30, are more accurate than the static algorithm based on longitudinal bending, but not as accurate as the algorithm based on transverse bending.

Table 9.30 – Accuracy classification for DB-WIM (Beam and Slab bridge) (R1)

(**n**: Total number of vehicles; **m**: mean; **s**: Standard deviation; $\mathbf{p_0}$: level of confidence; **d**: tolerance of the retained accuracy class; $\mathbf{d_{min}}$: minimum width of the confidence interval for π_0; **p**: Level of confidence of the interval $[-\delta,\delta]$)

	Relative error statistics				**Accuracy calculation**				
Criterion	**n**	**m (%)**	**s (%)**	**p_o (%)**	**Class**	**d (%)**	**d_{min} (%)**	**p (%)**	**Class Retained**
Single axle	55	0.79	8.95	91.6	C(15)	20	18.3	91.6	**C(15)**
Group of axles	27	0.17	8.22	89.1	C(15)	18	16.9	89.1	
Gross Weight	28	0.55	5.55	89.3	C(15)	15	11.5	89.3	

The MS-BWIM system measures longitudinal bending on the bottom slab deck of three different sections at 4.5, 9.5 and 14.5 m from the bridge start (in two transverse locations under the slow lane and fast lane at 2.0 m from the centreline). A system of six equations can be formulated at each instant: one relating transverse bending and another relating longitudinal bending for each one of the three instrumented sections (The longitudinal strain at each sensor in a section can be added together while the transverse bending is subtracted). However this arrangement fails to predict an instantaneous solution when there are three axles on the bridge. A new arrangement based purely on longitudinal bending of six sensors offers a solution for a small portion of the bridge. The results for this last arrangement are shown in Table 9.31. An overall accuracy B(10) is better than other algorithms based on longitudinal bending at one single location, but worse than the algorithm based on transverse bending at midspan.

Figure 9.31 shows the percentage of predicted weight over the static weight for different algorithms and criteria.

Table 9.31 – Accuracy classification for static MS-BWIM (Beam and Slab bridge) (R1)

(**n**: Total number of vehicles; **m**: mean; **s**: Standard deviation; $\mathbf{p_0}$: level of confidence; **d**: tolerance of the retained accuracy class; $\mathbf{d_{min}}$: minimum width of the confidence interval for π_0; **p**: Level of confidence of the interval $[-\delta,\delta]$)

	Relative error statistics				Accuracy calculation				
Criterion	**n**	**m (%)**	**s (%)**	**p_o (%)**	**Class**	**d (%)**	**d_{min} (%)**	**p (%)**	**Class Retained**
Single axle	27	0.33	2.08	92.1	**A(5)**	8	4.7	99.8	**B(10)**
Axle of group	18	-0.71	6.43	90.3	**B(10)**	20	14.5	98.1	
Group of axles	9	-0.38	1.32	83.4	**A(5)**	7.14	3.1	99.8	
Gross Weight	18	0.02	1.33	90.3	**A(5)**	5	3.0	99.5	

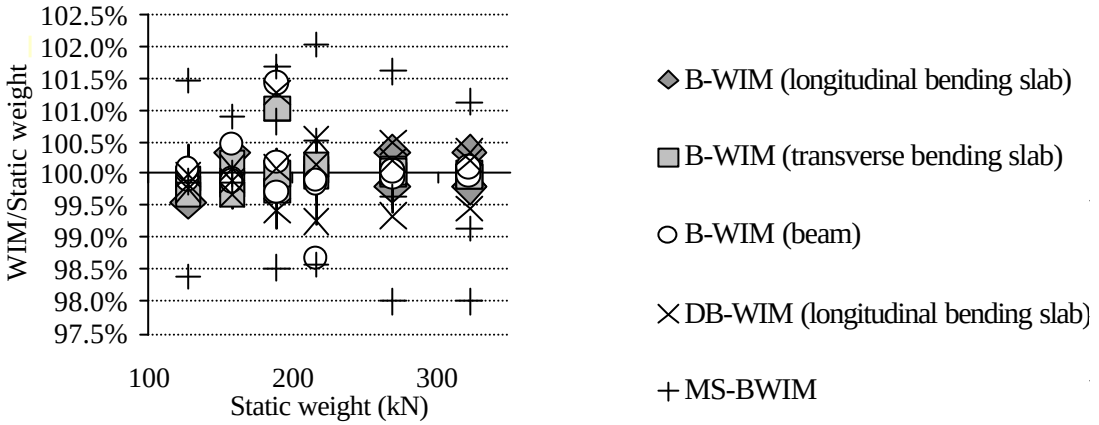

(a) Gross vehicle weight

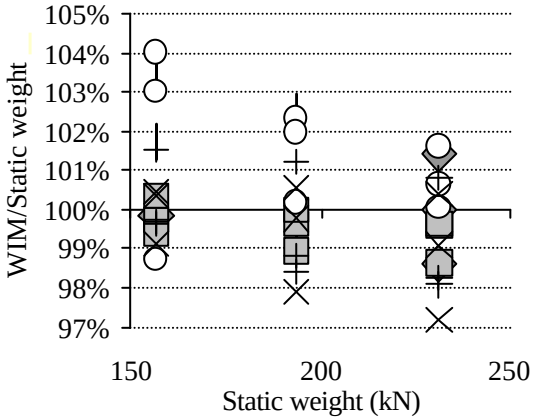

(b) Axle group

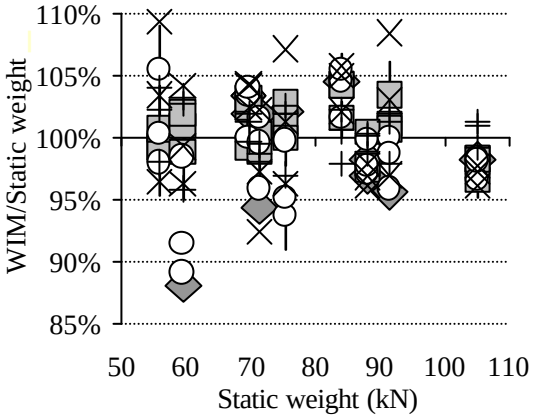

(c) Individual axle weights

Figure 9.31 – WIM/Static versus real static weights (Beam and slab)

9.3.6 Skew

Details of this 15 m bridge (first natural frequency 7.41 Hz) are given in Section 6.5.6. Dynamics are less significant than for the straight slab of the same length described in Section 9.3.1. However, a 45° skew can have a very negative influence on final results (Sections 3.2.2 and 3.7.2). Two sensors at 7.5 m from the bridge start and spaced 4 m symmetrically about the centreline are used as input for the static B-WIM algorithm. Table 9.32 shows how a global accuracy of E(50) is obtained (compared to C(15) in the straight slab). Accuracy classes A(5) and B+(7) are achieved for gross weight and group of axles criteria respectively.

Table 9.32 – Accuracy classification for static B-WIM algorithm (Skew bridge) (R1)

(**n**: Total number of vehicles; **m**: mean; **s**: Standard deviation; $\mathbf{p_0}$: level of confidence; **d**: tolerance of the retained accuracy class; $\mathbf{d_{min}}$: minimum width of the confidence interval for π_0; **p**: Level of confidence of the interval $[-\delta,\delta]$)

	Relative error statistics				Accuracy calculation				
Criterion	**n**	**m (%)**	**s (%)**	**p_0 (%)**	**Class**	**d (%)**	**d_{min} (%)**	**p (%)**	**Class Retained**
Single axle	27	-6.97	21.89	92.1	**E(50)**	60	50.6	96.7	**E(50)**
Group of axles	9	6.58	0.92	83.4	**B+(7)**	10	8.2	99.1	
Gross Weight	18	0.02	1.40	90.3	**A(5)**	5	3.2	99.3	

A dynamic algorithm based on the same sensors also gives poor results for single axle weights (Table 9.33).

Table 9.33 – Accuracy classification for dynamic B-WIM algorithm (Skew bridge) (R1)

(**n**: Total number of vehicles; **m**: mean; **s**: Standard deviation; $\mathbf{p_0}$: level of confidence; **d**: tolerance of the retained accuracy class; $\mathbf{d_{min}}$: minimum width of the confidence interval for π_0; **p**: Level of confidence of the interval $[-\delta,\delta]$)

	Relative error statistics				Accuracy calculation				
Criterion	**n**	**m (%)**	**s (%)**	**p_0 (%)**	**Class**	**d (%)**	**d_{min} (%)**	**p (%)**	**Class Retained**
Single axle	27	-9.07	19.20	92.1	**E(45)**	54	46.1	96.5	**E(45)**
Group of axles	9	9.36	1.84	83.4	**B(10)**	13	12.7	86.8	
Gross Weight	18	0.02	1.34	90.3	**A(5)**	5	3.0	99.5	

Strain is obtained in six different points at 3.5, 7.5 and 11.5 m from the bridge start in two transverse positions (under the slow and fast lane at 2.0 m from the centreline) are used for testing the MS-BWIM algorithm. These locations allow an instantaneous solution for the two-axle truck, but they fail to predict axles while there are three axles on the bridge and no accuracy classification can be provided. The limitations of the MS-BWIM are due to the characteristics of the influence lines for this choice of sensors. An instantaneous solution might be possible by using a higher number of sensors placed along the vehicle path (Section 7.5.2).

Though accuracy for individual axle weights is poor for the skewed bridge, there can be a reasonable prediction of gross weight as shown in Figure 9.32.

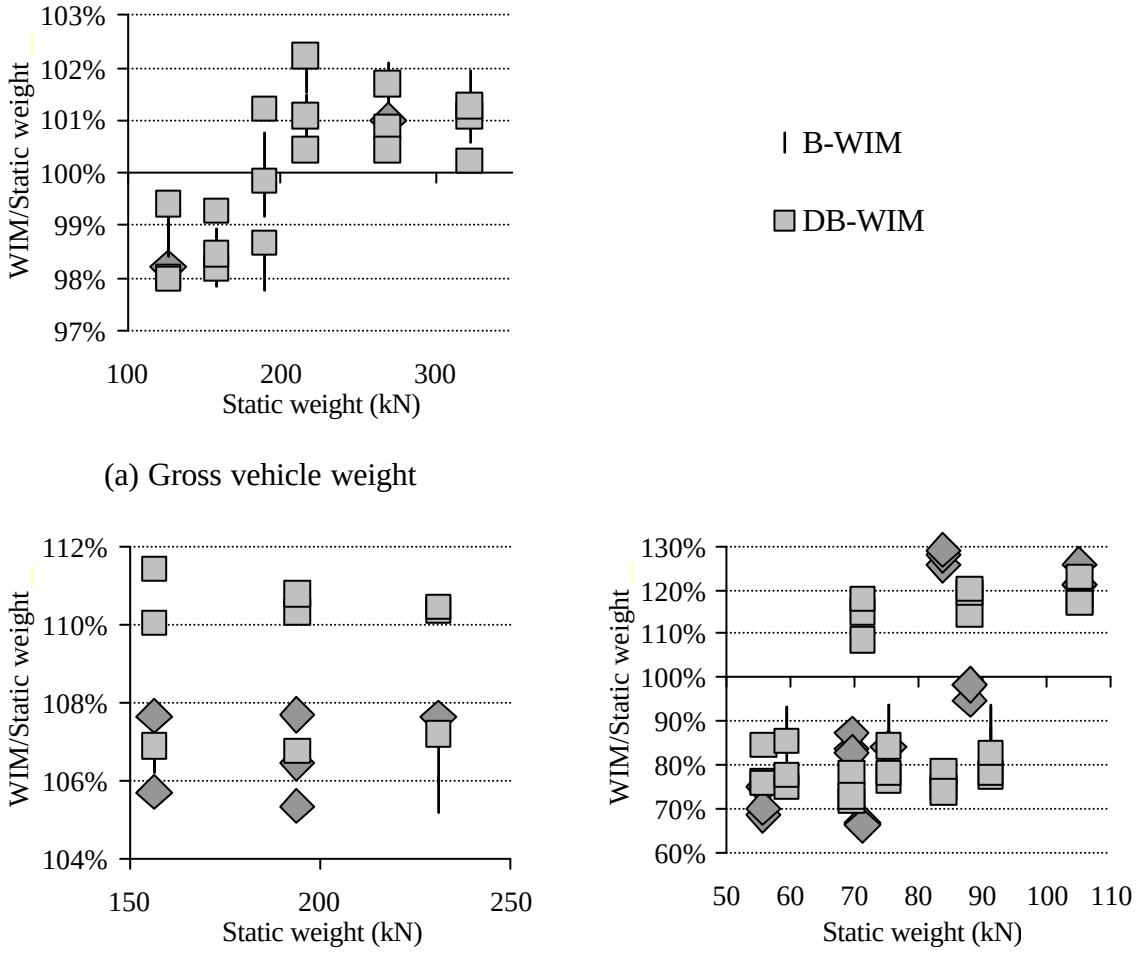

(a) Gross vehicle weight

(b) Axle group

(c) Individual axle weights

Figure 9.32 – WIM/Static versus static weights (Skew bridge)

9.3.7 Cellular

Details of this two span 62 m bridge (first natural frequency 2.95 Hz) are given in Section 6.5.7. Compared to the previous types of bridge, this is the longest and accuracy is expected to decrease (as mentioned in Section 3.2.2). It also has the lowest first natural frequency. The B-WIM algorithm based on one longitudinal location is tested initially with two sensors measuring longitudinal bending, and secondly with two sensors measuring transverse bending (all located under the bottom plate at midspan). The results of longitudinal bending at the sensors are added, but the transverse bending of both sensors is subtracted as their influence lines have opposite signs.

The use of transverse bending improves accuracy in individual axle weights from E(95) to E(30) (Tables 9.34 and 9.35). Transverse bending is not too influenced by other traffic far from the sensor location and it can be an alternative in long span bridges. GVW is determined more accurately by measuring longitudinal bending (smaller δ_{min}). A combination of transverse and longitudinal bending appears to be the best solution for this type of bridge behaviour.

Table 9.34 – Accuracy classification for static B-WIM (longitud. bending) (Cellular) (R1)
(**n**: Total number of vehicles; **m**: mean; **s**: Standard deviation; $\mathbf{p_0}$: level of confidence; **d**: tolerance of the retained accuracy class; $\mathbf{d_{min}}$: minimum width of the confidence interval for π_0; **p**: Level of confidence of the interval $[-\delta,\delta]$)

	Relative error statistics				**Accuracy calculation**				
Criterion	**n**	**m (%)**	**s (%)**	**p_o (%)**	**Class**	**d (%)**	**d_{min} (%)**	**p (%)**	**Class Retained**
Single axle	27	-0.92	8.39	92.1	**C(15)**	20	18.8	94.1	**E(95)**
Axle of group	18	-2.15	45.41	90.3	**E(95)**	119	102.3	95.1	
Group of axles	9	0.97	4.12	83.4	**B+(7)**	10	9.6	85.7	
Gross Weight	18	0.00	0.49	90.3	**A(5)**	5	1.1	100.	

Table 9.35 – Accuracy classification for static B-WIM (transver. bending) (Cellular) (R1)

(**n**: Total number of vehicles; **m**: mean; **s**: Standard deviation; $\mathbf{p_0}$: level of confidence; **d**: tolerance of the retained accuracy class; $\mathbf{d_{min}}$: minimum width of the confidence interval for π_0; **p**: Level of confidence of the interval $[-\delta,\delta]$)

	Relative error statistics				Accuracy calculation				
Criterion	**n**	**m (%)**	**s (%)**	**p_o (%)**	**Class**	**d (%)**	**d_{min} (%)**	**p (%)**	**Class Retained**
Single axle	27	0.42	4.02	92.1	**B+(7)**	11	9.0	97.1	**E(30)**
Axle of group	18	-0.26	17.15	90.3	**E(30)**	41	38.6	92.5	
Group of axles	9	-0.30	1.70	83.4	**A(5)**	7.14	3.9	99.1	
Gross Weight	18	0.01	0.90	90.3	**A(5)**	5	2.0	100.	

As in Section 9.3.2, the static B-WIM algorithm is tested with longitudinal bending at the central support. Results are given in Table 9.36. Overall accuracy is again better than at midspan (D+(20) compared to E(30)). Single axles are also one class better, but the Gross Weight is more accurately predicted by the longitudinal bending at midspan.

Table 9.36 – Accuracy classification for static B-WIM (central support) (Cellular) (R1)

(**n**: Total number of vehicles; **m**: mean; **s**: Standard deviation; $\mathbf{p_0}$: level of confidence; **d**: tolerance of the retained accuracy class; $\mathbf{d_{min}}$: minimum width of the confidence interval for π_0; **p**: Level of confidence of the interval $[-\delta,\delta]$)

	Relative error statistics				Accuracy calculation				
Criterion	**n**	**m (%)**	**s (%)**	**p_o (%)**	**Class**	**d (%)**	**d_{min} (%)**	**p (%)**	**Class Retained**
Single axle	27	-0.41	2.21	92.1	**A(5)**	8	5.0	99.6	**D+(20)**
Axle of group	18	-1.05	12.87	90.3	**D+(20)**	30	29.0	91.5	
Group of axles	9	0.51	1.12	83.4	**A(5)**	7.14	2.7	99.9	
Gross Weight	18	0.00	0.10	90.3	**A(5)**	5	2.0	100.	

The dynamic algorithm is tested with the longitudinal bending of two sensors placed at midspan. Accuracy classes in Table 9.37 are better than the static algorithm based on the same longitudinal strain (Table 9.34), but they are less accurate than transverse strain (Table 9.35) or the location at central support (Table 9.36).

Table 9.37 – Accuracy classification for DB-WIM algorithm (Cellular bridge) (R1)

(**n**: Total number of vehicles; **m**: mean; **s**: Standard deviation; $\mathbf{p_0}$: level of confidence; **d**: tolerance of the retained accuracy class; $\mathbf{d_{min}}$: minimum width of the confidence interval for π_0; **p**: Level of confidence of the interval $[-\delta,\delta]$)

	Relative error statistics				Accuracy calculation				
Criterion	**n**	**m (%)**	**s (%)**	**p_o (%)**	**Class**	**d (%)**	**d_{min} (%)**	**p (%)**	**Class Retained**
Single axle	27	0.73	4.43	92.1	**B+(7)**	11	10.0	94.9	**E(35)**
Axle of group	18	-0.27	19.21	90.3	**E(35)**	47	43.3	93.2	
Group of axles	9	-0.56	1.22	83.4	**A(5)**	7.14	3.0	99.9	
Gross Weight	18	0.00	0.50	90.3	**A(5)**	5	1.1	100.	

The MS-BWIM system measures longitudinal bending at twelve different points on the bottom slab deck (7.5, 15.5, 23.5, 31.5, 39.5 and 47.5 m from the bridge start in two transverse positions under the slow and fast lane at 2.5 m from the centreline. The results of these two transverse positions are added together at each section). The instantaneous calculation has a solution for only a very small portion of the bridge due to the long distance between sensors, which leads to the poor accuracy shown in Table 9.38.

Table 9.38 – Accuracy classification for static MS-BWIM algorithm (Cellular bridge) (R1)

(**n**: Total number of vehicles; **m**: mean; **s**: Standard deviation; $\mathbf{p_0}$: level of confidence; **d**: tolerance of the retained accuracy class; $\mathbf{d_{min}}$: minimum width of the confidence interval for π_0; **p**: Level of confidence of the interval $[-\delta,\delta]$)

	Relative error statistics				Accuracy calculation				
Criterion	**n**	**m (%)**	**s (%)**	**p_o (%)**	**Class**	**d (%)**	**d_{min} (%)**	**p (%)**	**Class Retained**
Single axle	27	-0.32	6.87	92.1	**C(15)**	20	15.3	98.2	**D(25)**
Group of axles	9	3.38	11.06	83.4	**D(25)**	28	26.0	87.2	
Gross Weight	18	0.32	6.15	90.3	**C(15)**	15	13.9	93.1	

The inaccuracy of MS-BWIM is mainly caused by the failure to predict axle group weight in two runs of the unloaded three-axle vehicle, as shown in Figure 9.33.

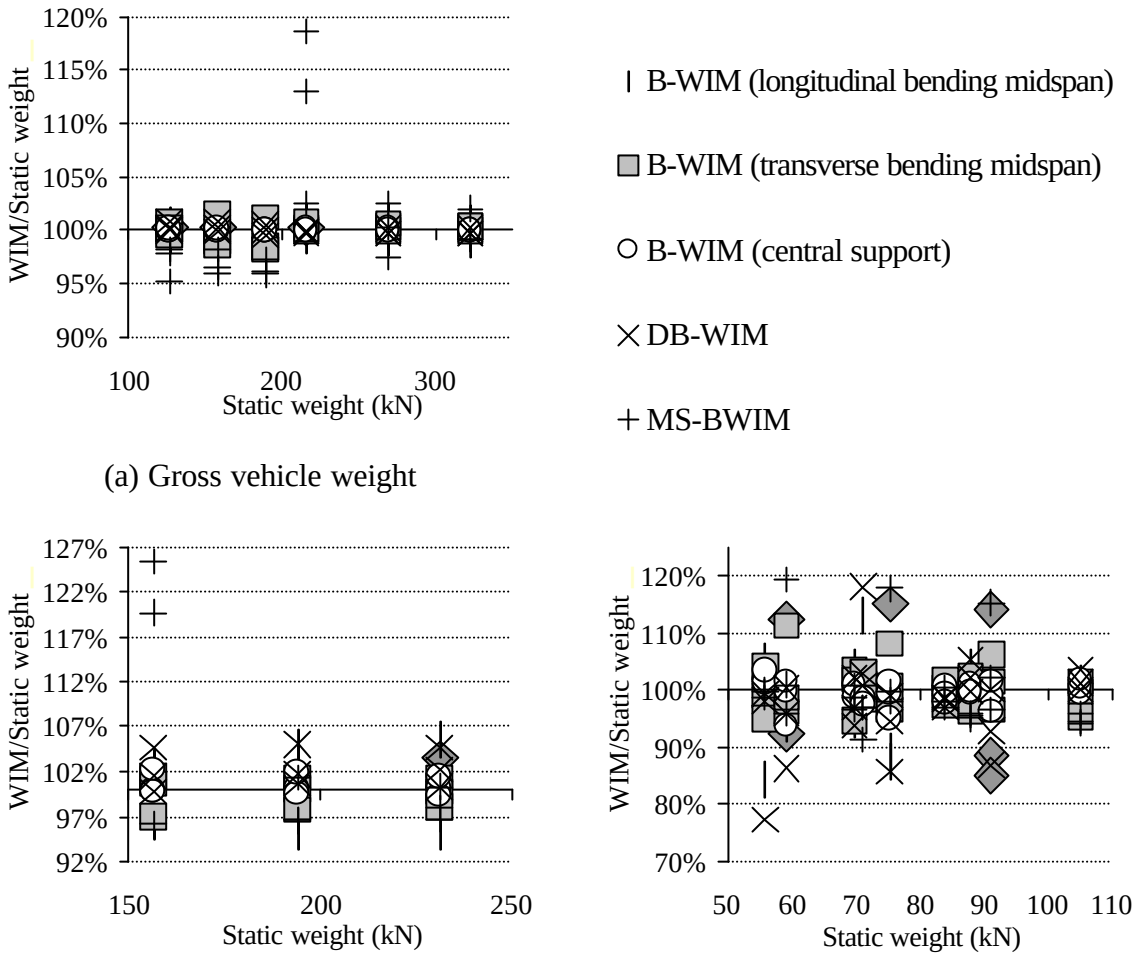

(a) Gross vehicle weight

(b) Axle group

(c) Individual axle weights

Figure 9.33 – WIM/Static versus real static weights (Two-span cellular bridge)

9.4 SUMMARY

This chapter has analysed the performance of three B-WIM algorithms on different bridges. The algorithms are:

- Static B-WIM algorithm based on one longitudinal location, as defined in Section 3.3,
- Dynamic B-WIM algorithm (DB-WIM) based on one longitudinal location, as defined in Section 7.3,
- Static multiple-sensor BWIM (MS-BWIM) algorithm as defined in Section 7.5.2.

Other algorithms such as the spectral approach in Section 7.2 or the dynamic MS-BWIM algorithm in Section 7.5 have not been considered. It was found that the first algorithm did not give good results when having more than two axles on a bridge (Section 7.2.5).

Compared to the dynamic MS-BWIM algorithm, the static version of the multiple sensor system was preferred because the static B-WIM algorithm has generally been more accurate than DB-WIM and it involves fewer parameters (both one-sensor and multiple-sensor algorithms are based on the same equations).

First, a beam model was analysed. The system was calibrated with a two-axle linear sprung vehicle and tested with a four-axle non-linear sprung vehicle (11 degrees of freedom). Air and steel suspensions on both smooth and rough pavements were considered. In smooth road conditions, MS-BWIM achieved the most accurate overall class B+(7) (corresponding to the criterion of individual axle weights). The traditional static B-WIM had the same accuracy class, A(5), for gross vehicle weight as MS-BWIM, but it failed to predict individual axle weights accurately (E(45)). The 30 m span length makes it difficult to identify individual axles from strain at only one location, and MS-BWIM derives a more accurate value from the load history. DB-WIM was the most inaccurate system regardless of the criterion adopted. The performance of DB-WIM improves when considering air suspensions, but it can not cover for different dynamic behaviours. DB-WIM approximates the total strain with a particular dynamic model (i.e., based on moving constant loads). If this approximation is not good, then an averaging of all dynamics, as carried out in the static algorithm, gives better results.

The poorest results were obtained with steel suspensions on rough profiles. The truck forces in the steel-sprung vehicle are excited more strongly than in the air-sprung model (heavily damped). Bridge strains also oscillate with higher amplitudes when crossed by the steel suspension truck. This is probably due to the proximity of the frequencies of the truck and the bridge, which results in huge errors in any B-WIM algorithm. In these conditions, the estimation of individual axle weights is very inaccurate, but the traditional static B-WIM algorithm can still provide reasonable values for gross vehicle weight (C(15)). The explanation is twofold:

- Averaging the effect of dynamics caused by the traditional static algorithm (more accurate than the dynamic modelling of the total strain as attempted by the DB-WIM algorithm),
- Sensor location at midspan (MS-BWIM considers other sensor locations which are not as accurate and this results in higher errors).

Results for the beam model are summarised in Table 9.39 under limited reproducibility conditions.

Table 9.39 - Accuracy results for Green's simulations

Road profile	Criterion	One longitudinal location algorithms		Static Multiple-Sensor
		Static	Dynamic	
Smooth	Single axle	E(45)	E(65)	B+((7)
	Group of axles	C(15)	E(30)	A(5)
	Gross weight	A(5)	B+(7)	A(5)
	Overall	E(45)	E(65)	B+(7)
Rough	Single axle	E(300)	E(395)	E(30)
	Group of axles	E(100)	E(130)	E(50)
	Gross weight	C(15)	E(50)	E(30)

The performance of B-WIM on a 16 m long isotropic slab has been considered. All three algorithms have achieved class A(5) for gross vehicle weight. The traditional static algorithm based on the midspan location has reached an overall class of C(15). When increasing the number of sensors at midspan from 2 to 8, the system has remained in the same class for each criterion. DB-WIM has also reached class C(15) overall. MS-BWIM has provided an overall accuracy class of A(5). MS-BWIM calculates individual axles more accurately than any other algorithm. When the lateral truck position was changed, there was no loss in accuracy.

In a two-span isotropic slab (total length 37 m), it was found that the best location for weighing is at the central support. The static B-WIM algorithm achieves an overall accuracy of A(5) at the central support location, while only D+(20) is reached at midspan. MS-BWIM also provides A(5) accuracy overall. DB-WIM is in class B(10) overall using strain at midspan, better than D+(20) using the static algorithm at the same location. This is a case where the approximation of the total strain by a dynamic model results in better accuracy than approximating the static response. DB-WIM might be preferred if the central support is not accessible. However, only a reduced number of truck configurations were tested: four-axle articulated vehicle in the beam model and two- and three-axle rigid vehicle in the finite element models. The testing of more trucks will allow a more realistic accuracy threshold for the site under study to be determined.

A slab with edge cantilever (20 m long) has resulted in class A(5) for gross vehicle weight or axle group for any of the B-WIM algorithms under study. A(5), B(10) and C(15) were obtained for individual axle weights using MS-BWIM, static B-WIM and DB-WIM respectively. The dynamic oscillations of this bridge were small, and the static version of the algorithm (based on one or multiple sensors) gave better results than trying to model those oscillations by DB-WIM.

A voided slab deck (25 m) bridge has also been tested. The first natural frequency is relatively low (3.80 Hz) and dynamic oscillations have higher amplitudes than in the preceding slab with edge cantilever. In this case, DB-WIM achieves an overall accuracy class C(15), better than D(25) using the static algorithm or D+(20) using MS-BWIM. MS-BWIM achieves poorer results for gross weight (C(15)) than the other two algorithms (A(5)). For the combination of sensors chosen in this bridge, the instantaneous calculation by MS-BWIM is only feasible for a very small portion of the bridge (for a small part of the strain record) and the estimation of gross weight is poor. The algorithms based purely on one longitudinal location obtain the gross vehicle weight more accurately as they use all strain readings along the bridge. Therefore, DB-WIM appears to approximate the total strain very accurately, though the algorithm should be tested with other truck configurations.

A beam and slab (20 m long) bridge has been tested. When applying the static B-WIM algorithm to the response of this bridge, it has been found that transverse bending can provide a more accurate estimation of weights than longitudinal bending (overall accuracy class A(5) for transverse bending compared to B+(7) for longitudinal bending at midspan). MS-BWIM is in class A(5). DB-WIM can only achieve C(15).

Results for a 45º skew bridge (15 m long) were poor, except for gross vehicle weight and group of axles. The sensors chosen for the MS-BWIM did not allow for an instantaneous calculation. Further study on the ideal number and location of multiple sensors is required.

Finally, a two-span cellular bridge (62 m long) was tested. As in the other two-span continuous bridge, best results are obtained when using the static B-WIM algorithm at the central support (overall accuracy class A(5)). If using strain at midspan, the static algorithm based on transverse bending achieves B+(7), compared to C(15) if based on

longitudinal bending. DB-WIM reaches B+(7) when applied to longitudinal bending at midspan. The span is too long for the reduced number of sensors chosen for the MS-BWIM system, and an instantaneous calculation can only take place for a short period of time. Hence, MS-BWIM falls in overall accuracy class D(25).

Table 9.40 summarises accuracy results for different algorithms based on longitudinal strain and finite element simulations under limited reproducibility conditions.

Table 9.40 - Accuracy results for finite element models

Bridge type	**Criterion**	**One longitudinal algorithms based on location at midspan**		**Static Multiple-Sensor**
		Static	**Dynamic**	
Isotropic slab	Single axle	C(15)	C(15)	A(5)
	Group of axles	B+(7)	B+(7)	A(5)
	Gross weight	A(5)	A(5)	A(5)
	Overall	C(15)	C(15)	A(5)
Two span isotropic slab	Single axle	D+(20)	B(10)	A(5)
	Group of axles	B+(7)	A(5)	A(5)
	Gross weight	A(5)	A(5)	A(5)
	Overall	D+(20)	B(10)	A(5)
Slab with edge cantilever	Single axle	B(10)	C(15)	A(5)
	Group of axles	A(5)	A(5)	A(5)
	Gross weight	A(5)	A(5)	A(5)
	Overall	B(10)	C(15)	A(5)
Voided slab deck	Single axle	D(25)	C(15)	C(15)
	Group of axles	C(15)	B+(7)	D+(20)
	Gross weight	A(5)	A(5)	C(15)
	Overall	D(25)	C(15)	D+(20)
Beam and slab	Single axle	B+(7)	C(15)	A(5)
	Group of axles	A(5)	C(15)	A(5)
	Gross weight	A(5)	C(15)	A(5)
	Overall	B+(7)	C(15)	A(5)
Skew	Single axle	E(50)	E(45)	-
	Group of axles	B+(7)	B(10)	-
	Gross weight	A(5)	A(5)	-
	Overall	E(50)	E(45)	-
Two span Cellular	Single axle	C(15)	B+(7)	C(15)
	Group of axles	B+(7)	A(5)	D(25)
	Gross weight	A(5)	A(5)	C(15)
	Overall	C(15)	B+(7)	D(25)

The static algorithm can produce different accuracy classes depending on the strain type and location. Table 9.41 gives accuracy results for strains other than longitudinal bending at midspan.

Table 9.41 - Accuracy results for static algorithm based on one longitudinal location and different type of strains

Bridge type	**Strain**	**Single axle**	**Group of axles**	**Gross weight**	**Overall**
Two span isotropic slab	Longitudinal bending at midspan	D+(20)	B+(7)	A(5)	D+(20)
	Longitud.bending at central support	A(5)	A(5)	A(5)	A(5)
Beam and slab	Longitudinal bending of beam	B+(7)	A(5)	A(5)	B+(7)
	Longitudinal bending of slab	B+(7)	A(5)	A(5)	B+(7)
	Transverse bending of slab	A(5)	A(5)	A(5)	A(5)
Two span Cellular	Longitudinal bending at midspan	C(15)	B+(7)	A(5)	C(15)
	Transverse bending at midspan	B+(7)	A(5)	A(5)	B+(7)
	Longitud. bending at central support	A(5)	A(5)	A(5)	A(5)